THESIS FOR THE DEGREE OF LICENTIATE OF ENGINEERING

Dynamic Modeling and Simulation of SAG Mill Circuits with Pebble Crushing

Haijie Li

Department of Industrial and Materials Science

CHALMERS UNIVERSITY OF TECHNOLOGY

Gothenburg, Sweden 2020

Dynamic Modeling and Simulation of SAG Mill Circuits with Pebble Crushing

Haijie Li

Technical report No. IMS-2020-2

Department of Industrial and Materials Science

Chalmers University of Technology

SE-412 96 Gothenburg

Sweden

Telephone + 46 (0)31-772 1000

Cover:

Picture shows two ball mills and one SAG mill taken from www.flsmidth.com

Printed by

Chalmers Reproservice

Gothenburg, Sweden 2020

Abstract

Grinding is one of the most energy-consuming processes in the mining industry. As a critical part of the comminution process, autogenous grinding (AG) or semi-autogenous grinding (SAG) mills are often used for primary grinding. However, the breakage mechanism of an AG/SAG mill is inefficient in grinding particles of a certain size, typically in the range of 25-55 mm, i.e., pebbles. Therefore, cone crushers are often used as pebble crushers and integrated into AG/SAG mill circuits to break the critical size particles that accumulate in the mill and to increase the performance of the primary grinding circuits.

Many studies have been carried out, mainly focusing on optimizing of SAG mills and cone crushers, respectively, but only a few have investigated the dynamic interactions between a SAG mill and its pebble crushers. The scope of this thesis is to examine the dynamic relations between the SAG mill and the pebble crusher in a closed circuit and thus to optimize the circuit efficiency by controlling the pebble crusher operational settings.

In this thesis, two modeling techniques are proposed for simulating the dynamics in the grinding process. The first method is the fundamental modeling method, where the underlying physics of the comminution process has been considered. The proposed mill model is divided into sub-processes that include breakage behavior in each sub-division, particle transportation within the mill chamber, and the discharge rate from the mill. The dynamic cone crusher model describes the crusher chamber as a surge bin and predicts the product particle sizes based on crusher CSS and eccentric speed. In the simulation model, other production units such as screens and conveyors are included to describe the dynamics of the circuit better. The flexibility of this method allows one to apply this simulation library to a variety of plants with different configurations.

The second modeling technique presented in this study is based on data-driven methods, where two SAG mill power models are developed. The first model calculates the mill power draw by combining several individual data-driven algorithms. The second model uses historical data to forecast the mill power draw in advance. These data-driven methods can make high accuracy predictions based on a specific plant dataset, and find complex nonlinear relations between input variables and target outputs.

The results from both simulations and industrial data analysis show that significant dynamic impact can be induced by altering the pebble crusher operational settings. Therefore, the performance (throughput or specific energy) of an AG/SAG closed circuit can be improved with the optimized utilization of its recycle pebble crusher. While the present work is based on simulation and analysis of plant data, full-scale tests and further model development are needed as part of a future study.

Keywords: Dynamic modeling, AG/SAG mill, Cone crusher, Pebble crushing, Fundamental modeling method, Data-driven modeling method, Comminution process

Acknowledgements

This thesis was carried out at the Chalmers Rock Processing System research group at the Department of Industrial and Materials Science, Chalmers University of Technology. This work is jointly funded by FLSmidth A/S and the Innovation Fund Denmark.

First of all, I would like to express my gratitude to my supervisors Prof. Magnus Evertsson, Dr. Gauti Asbjörnsson, and Dr. Erik Hulthén for the careful guidance, the share of knowledge and constant support during the past two and half years. I gratefully appreciate and acknowledge the support received from my company supervisor Dr. Mats Lindqvist for his valuable suggestions and inspirations both in academic study and daily life.

I'd like to thank all colleagues at Global R&D, Minerals Division at FLSmidth A/S and the colleagues at Chalmers Rock Processing Systems research group.

Finally, I'd like to express special thanks to my girlfriend Haomin and my family for all the love and joy they bring to me.

Haijie Li

Copenhagen, January 2020

List of Publications

Appended papers:

Paper A.

Li, Haijie, Magnus Evertsson, Mats Lindqvist, Erik Hulthén, and Gauti Asbjörnsson. *Dynamic modelling and simulation of an AG/SAG mill with multi component ore*, presented in proceedings of IMPC 2018 – 29th International Mineral Processing Congress, Moscow, September 2018.

Paper B.

Li, Haijie, Magnus Evertsson, Mats Lindqvist, Erik Hulthén, and Gauti Asbjörnsson. *Dynamic modeling and simulation of a SAG mill-pebble crusher circuit by controlling crusher operational parameters*. Minerals Engineering 127 (2018): 98-104.

Paper C.

Li, Haijie, Magnus Evertsson, Mats Lindqvist, Erik Hulthén, Gauti Asbjörnsson and Graham Bonn, *Dynamic modelling of a SAG mill – pebble crusher circuit by data-driven methods*, presented in proceedings of SAG conference 2019, Vancouver, September 2019.

Paper D.

Li, Haijie, Magnus Evertsson, Mats Lindqvist and Gauti Asbjörnsson, *A data-driven method to isolate the effect of pebble recycling on AG/SAG mill circuit.* To be presented in Comminution 2020, Cape Town, April 2020.

Work distribution:

Paper A.

Li and Evertsson initiated the idea, Li developed the model with support from Asbjörnsson, Li wrote the paper, Evertsson and Hulthén as reviewers.

Paper B.

Li and Lindqvist initiated the idea, Li developed the model with support from Evertsson and Asbjörnsson, Li wrote the paper, Evertsson and Hulthén as reviewers.

Paper C.

Li initiated the idea, Li implemented the code with dataset from Bonn, Li wrote the paper with Evertsson, Asbjörnsson and Lindqvist reviewers.

Paper D.

Li initiated the idea, Li wrote the paper with Evertsson, Asbjörnsson and Lindqvist as reviewer.

Table of Contents

List of Abbreviations

AG	Autogenous mill
ANN	Artificial neural network
CNN	Convolutional neural network
CPA	Change point analysis
CRPS	Chalmers Rock Processing Systems
CSS	Closed side settings
DEM	Discrete element method
FC	Fully connected layers
GBR	Gradient boosting regression
IAM	Integrated analysis method
JKMRC	The Jullius Kruttschnitt Mineral Research Center
KNN	K-nearest neighbors
LSTM	Long short-term memory
PBM	Population balance method
PSD	Particle size distribution
RF	Random forest
RNN	Recurrent neural network
SAG	Semi-autogenous mill
SE	Specific energy

List of Figures

1 INTRODUCTION

The aim of this chapter is to:

- Introduce the background and hypothesis of the research project.
- Introduce the research scope and research questions.

1.1 Background and Problem Statement

The AG/SAG mill was invented in the late 1950s and was quickly implemented and dominates in the primary grinding process (Napier-Munn et al., 1996). The comminution process is one of the most energy-intensive processes in the minerals industry. Studies show that the comminution process consumes approximately 2% of the annual global electricity consumption (Fuerstenau and Han, 2003). It is also reported by Haque (Haque, 1999) that the energy consumption of AG/SAG mills (including operating power and the energy used during the mill components production procedures) accounts for 50% of the minerals industry, and the efficiency of grinding equipment can be as low as 1%. Therefore, efforts have been devoted during the past decades to increase the grinding process efficiency.

The word 'autogenous' in AG mills indicates the grinding media is formed exclusively by ore particles. In a SAG mill, external grinding balls are added in the chamber to aid in the grinding process. Napier-Munn (Napier-Munn et al., 1996) classified the breakage mechanisms occurring within AG/SAG mills into three categories: high energy related impact breakage, low energy related abrasion, and attrition. Due to the AG/SAG mill inherent breakage mechanism, particles of a size in the range of 25-55 mm (so-called critical size fraction) are not easily broken thoroughly and are likely to accumulate in the mill charge (Yu, 2017). The buildup of critical particles in a mill consumes a remarkable amount of power and leads to a lower mill throughput. Therefore, these pebble-sized particles need to be discharged from the mill and then addressed by an external crusher, usually a cone crusher (Johnson et al., 1994).

To gain a better understanding of the comminution process, and for the purpose of control and optimization, many approaches have been developed for the modeling of AG/SAG mills. These methods include empirical black-box modeling (Morrell, 1996), fundamental dynamic modeling (Jnr and Morrell, 1995, Kojovic et al., 2012, Yu et al., 2014), discrete element method

(de Carvalho, 2013, Morrison and Cleary, 2004), and data-driven methods (Xing-yu et al., 2017, Hoseinian et al., 2017). Similarly, many studies on modeling cone crushers have been conducted, including a fundamental breakage cone crusher model proposed by Evertsson (Evertsson, 2000), cone crusher wear dynamics modeling by Lindqvist (Lindqvist and Evertsson, 2006), active speed control algorithm by Hulthén (Hulthén, 2010) for cone crushers, and DEM breakage modeling method (Quist and Evertsson, 2016, Delaney et al., 2015).

However, these models mainly have focused on the optimization of mills and cone crushers respectively, but few have considered the connections of these two machines and investigated them as a whole system. The power draw of a big SAG mill can be up to 20 MW, while its pebble crusher power draw is usually only 300 to 1000 kW. It needs to be mentioned that the recycling load occupies around 20% of the total SAG mill throughput and up to 50% in an AG mill circuit (data based on the author's observations from FLSmidth customer plants). Moreover, Evertsson and Powell reported a generally poor utilization of pebble crushers in many grinding circuits (Powell et al., 2019).

The hypothesis of this research can thereby be summarized as follows:

In addition to the individual optimizations on AG/SAG mills and cone crushers, the performance of the grinding circuit can be improved by the pebble crusher selection (in the circuit designing phase) and by active control of the cone crusher (in the operating process).

1.2 Research Scope and Research Questions

The overall objective of this thesis is to investigate the dynamic interactions between a SAG mill and its pebble crusher, in order to enhance the circuit efficiency by increasing the total throughput or reducing the specific energy consumption. Approaches are proposed to develop high fidelity dynamic models of the AG/SAG mill, the cone crusher, and other units in the grinding circuit. Furthermore, validations with industrial tests need to be carried out for future circuit design and optimization.

The objectives of this work can be formulated by the following research questions:

RQ 1: What are the dynamic interactions between the SAG mill and the pebble crusher in a grinding process?

RQ 2: What approach can be used to model these interactions and other internal dynamics for SAG mills and pebble crushers?

RQ 3: How can these approaches be adapted and implemented in industrial applications?

2 RESEARCH APPROACH

The aim of this chapter is to:

- Describe the research methodology applied in this thesis.

2.1 Research Methodology

The research methodology used in this thesis has been proposed and used by Chalmers Rock Processing Systems (CRPS) research group in several research projects during the last two decades. The group is a part of the Division of Product Development at the Department of Industrial and Materials Science at Chalmers University of Technology. The proposed problem-oriented research approach was initially proposed by Evertsson (Evertsson, 2000) for developing new knowledge focusing on the problem itself. Asbjörnsson (Asbjörnsson, 2015) adopted this problem-oriented research approach and integrated it into a broad scope to include system development. The description of the approach is illustrated in Figure 1.

Projects carried out at CRPS are initiated and formulated from an identified industrial problem or knowledge gap with industrial relevance. After the problem formulation, systematic investigations are conducted, such as literature studies, initial experiments, interviews, and industrial data analysis. After the initial study, the next task was to select a suitable research method, as shown in Figure 1, the system-building phase. This problem-oriented research focuses on solving the problem based on the nature of the problem itself. Therefore, different methods can be compared and verified with respect to the modeling fidelity. This iterative process continues until the chosen methods show adequate performance on system modeling accuracy and suitability to a number of future applications. The last step after system building is validation, where case studies are applied to evaluate the modeling methods further. An early implementation during the research phase, as mentioned by Hulthén (Hulthén, 2010), provides additional insights into the examined system. Moreover, new problems could arise in the implementation step before the final industrial-scale application.

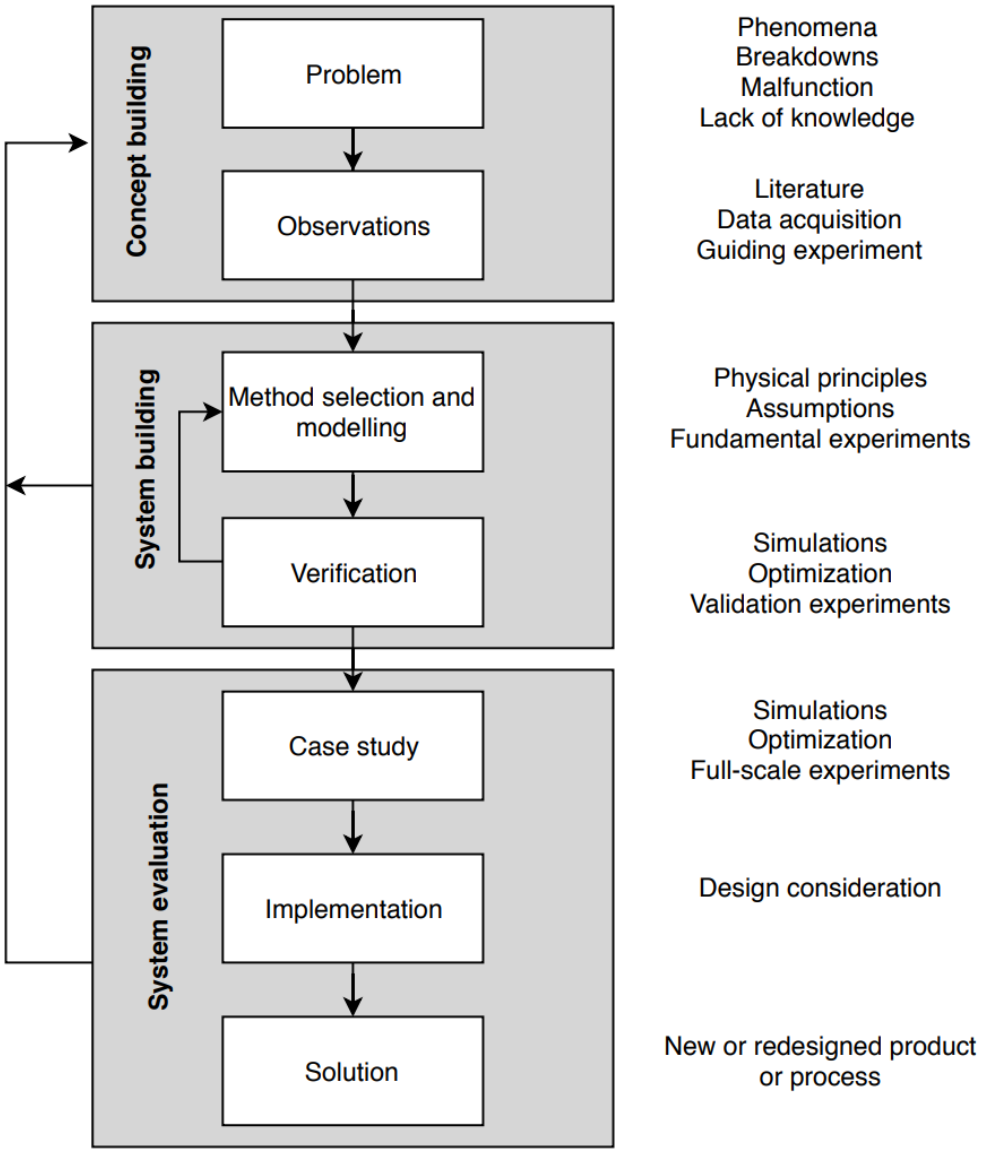

Figure 1. The applied problem-oriented research methodology based on Evertsson (Evertsson, 2000) and modified by Asbjörnsson (Asbjörnsson, 2015)

3 LITERATURE REVIEW

The aim of this chapter is to:

- Introduce research that has been focused on AG/SAG mill dynamic modeling and cone crusher modeling.
- Provide recent research on data-driven methods in the minerals industry.

3.1 Fundamental Models

Morrell divided SAG mill modeling methods into two groups: black-box models and mechanistic models (Napier-Munn et al., 1996). The black-box models do not normally represent the fundamental physics in the comminution process. This type of modeling technique is mainly derived from statistical results based on industrial data. The advantages include simplicity, low computational power, and good prediction for a specific device (Yu, 2017). The drawbacks of black-box models are that they are only useful within the defined boundary, depend on trained data, and offer limited generality at different plants.

The fundamental model is a type of model where the underlying physics of the comminution process is involved. A fundamental model considers ore breakage behavior and the interactions between the particles and elements in a mill (Napier-Munn et al., 1996). The advantage of a fundamental model compared to a black-box data-driven model is the wider application, such as advanced control and optimization for new devices. Sometimes the fundamental models in the area of comminution (crushing, screening, grinding, classification) are called mechanistic models.

3.1.1 SAG mill modeling

Morrell proposed a simplified structure for AG/SAG mills, in which three main components are used to describe the grinding dynamics (Morrell, 1992):

- Collision frequency (breakage rate)
- Ore size distribution after collision (appearance distribution function)

- Particle transport out of the mill

For a steady-state situation with the perfect mixing mass balance model, the grinding process within a mill can be summarized as follows as proposed by Whiten (Whiten, 1974):

$$0 = f_i - p_i + \sum_{j=1}^{i} r_j s_j a_{ij} - r_i s_i \tag{3.1}$$

$$p_i = d_i s_i \tag{3.2}$$

Where f_i is feed rate of particles of size i; p_i is product rate of particles of size i; r_i is breakage rate of particles of size i; s_i is mill contents of particles of size i; a_{ij} is appearance function, size class i breaks from size class j; d_i is discharge rate of size class i.

Based on the steady-state population balance method (PBM) as seen in Equation (3.1) and Equation (3.2), Valery and Morrel (Jnr and Morrell, 1995) proposed a dynamic mill model that calculates dynamic responses in terms of mill charge level, slurry level, mill power draw, feed ore size, and water addition:

$$\frac{ds_i(t)}{dt} = f_i - p_i + \sum_{j=1}^{i-1} r_j s_j a_{ij} - \left(r_i s_i - r_i s_i a_{ij} \right) \tag{3.3}$$

$$p_i = d_i s_i \tag{3.4}$$

Where $s_i(t)$ is the mass of particles in the mill of size i at time t.

Most recently, Yu (Yu, 2017) developed an integrated, mechanistic dynamic mill model based on the population balance framework and incorporates a full breakage function along with material characteristic depended appearance function, slurry transport functions, and discharge function.

In this integrated framework, the appearance function is taken from an updated JKMRC appearance function (Kojovic et al., 2012), which involves the size-dependent parameters as shown below:

$$t_{10} = M\left[1 - e^{-F_{mat} \cdot X \cdot E_{cs}}\right] \tag{3.5}$$

$$A \cdot b = 3600 \cdot M \cdot F_{mat} \cdot X \tag{3.6}$$

Where, t_{10} is breakage index, defined as the percentage passing one tenth of the original mean particles size, A and b are the ore breakage parameters determined from drop weight tests, E_{cs} is the specific comminution energy, M is the maximum possible value of t_{10} in impact, F_{mat} is material property relates to the ore-specific constants, X is the average particle size. The parameters in the appearance equations are determined by the drop weight test.

The breakage rate function is back-calculated (Kojovic et al., 2012) with a simplified PBM equation which it can be obtained under the assumption of perfect steady-state mixing:

$$f - R \cdot s + A \cdot R \cdot s - D \cdot s = 0 \tag{3.7}$$

Where f is feed rate; R is breakage rate; s is mill content; D is discharge rate; A is appearance function.

The discharge function is expressed as:

$$d_i^* = d_i\left(D^2 L\right)/4Q \tag{3.8}$$

$$d_i = d_{max} c_i \tag{3.9}$$

In the above equations, d_i is the discharge rate of size class i; d_i^* is the normalized discharge rate; D is the mill diameter; L is the mill length; Q is the volumetric flowrate; c_i is the classification function value for size class i.

The mill power draw in Yu's framework is from Morrell's empirical power model (Morrell, 1996):

$$P_{total} = Noload\ power + \left(KD^{2.5} L_e \rho_c \alpha \delta\right) \tag{3.10}$$

$$P_{idle} = 1.68 D^{2.05} [\phi\left(0.667 L_d + L\right)]^{0.82} \tag{3.11}$$

Where D is the diameter of the cylindrical section of the mill inside liners; K is the lumped parameter used in the calibration of the model. L is the length of the cylindrical section of the mill inside liners; L_d is the length of cone-end; L_e is the effective grinding length; α is an empirical parameter; ϕ is the fraction of critical speed; ρ_c is the density of total charge.

3.1.2 Cone crusher modeling

Cone crushers are widely used in aggregate production and in the mining industry. Evertsson (Evertsson, 2000) proposed a cone crusher model where the laws of mechanics and rock breakage characteristics are concerned. The corresponding mathematical expressions for single particle and interparticle breakage are is given in Equation (3.12) and (3.13):

$$\mathbf{P}_i = \left[\left[\mathbf{B}_i^{inter}\ \boldsymbol{S}_i + \left(\mathbf{I} - \boldsymbol{S}_i\right)\right]\mathbf{M}_i^{inter} + \mathbf{B}_i^{single}\mathbf{M}_i^{single}\right]\mathbf{P}_{i-1} \tag{3.12}$$

$$\mathbf{M}_i^{inter} + \mathbf{M}_i^{single} = \mathbf{I} \tag{3.13}$$

In Equation (3.12), $\mathbf{P}_i$ is the product size distribution from crushing zone i and $\mathbf{P}_{i-1}$ represents the product from the previous crushing zone; $\mathbf{B}_i$ is the breakage matrix and $\mathbf{S}_i$ is the selection matrix; the $\mathbf{M}_i$ matrix represents the proportion between single particle and interparticle breakage in a crushing zone and the sum of them should be an identity matrix $\mathbf{I}$.

Evertsson also introduced the cone crusher capacity calculation by integrating the mass-flow field over a horizontal cross-section of the crushing chamber. The mass flow is divided into the downward direction and the upward direction in Equation (3.14) and (3.15):

$$Q_{down} = \int_0^{\alpha_c} \int_{R_i(\alpha)}^{R_0} \rho v(\alpha) r dr d\alpha \tag{3.14}$$

$$Q_{up} = \frac{1}{2} \int_{\alpha_c}^{2\pi} \int_{R_i(\alpha)}^{R_0} \rho v(\alpha) r dr d\alpha \tag{3.15}$$

The overall capacity is calculated, as shown below:

$$Q = \eta_v \left(Q_{down} - Q_{up} \right) \tag{3.16}$$

Where R_i is the mantle radius; R_0 is the concave radius; α is the angle; v is the velocity vector; ρ is the bulk density of the material; η_v is a volumetric filling ratio.

However, as mentioned by Asbjörnsson (Asbjörnsson, 2015), the Evertsson crusher model is computationally heavy and needs a considerable amount of calculation time as the proposed model requires more detailed information, such as chamber geometry and breakage behavior.

3.2 Data-driven Models

As an alternative to the physics-based fundamental methods, and due to the wide use of new measurement technologies and distributed control systems, the data collection and data analysis in an industrial process are becoming more important (Ge et al., 2013). In minerals engineering, machine learning and data-driven techniques have drawn the attention of many researchers in recent years (Ding et al., 2017, Tang et al., 2010). Data-driven models can be used in developing soft sensors for mill load (Tang et al., 2012); plant monitoring and fault diagnosis (Horn et al., 2017); mill dynamic modeling (Hoseinian et al., 2017), and flotation froth analysis (Xing-yu et al., 2017). McCoy did a literature review of machine learning used in minerals processing (McCoy and Auret, 2019) over the past few decades. He suggested that a combination of the following factors is essential for the mineral processing engineers of tomorrow:

- Large quantities of diverse data with good quality
- Mineral processing expertise
- In-depth knowledge and extensive experience of the data analysis
- Computational thinking

Ge (Ge, 2017) proposed a general framework of the data-driven modeling for the plant-wide process, where its subsections including process decomposition, data-preprocessing, features and sample selection, model training, and real-time online process monitoring. In Figure 2, the flowchart of the data-driven modeling structure is illustrated.

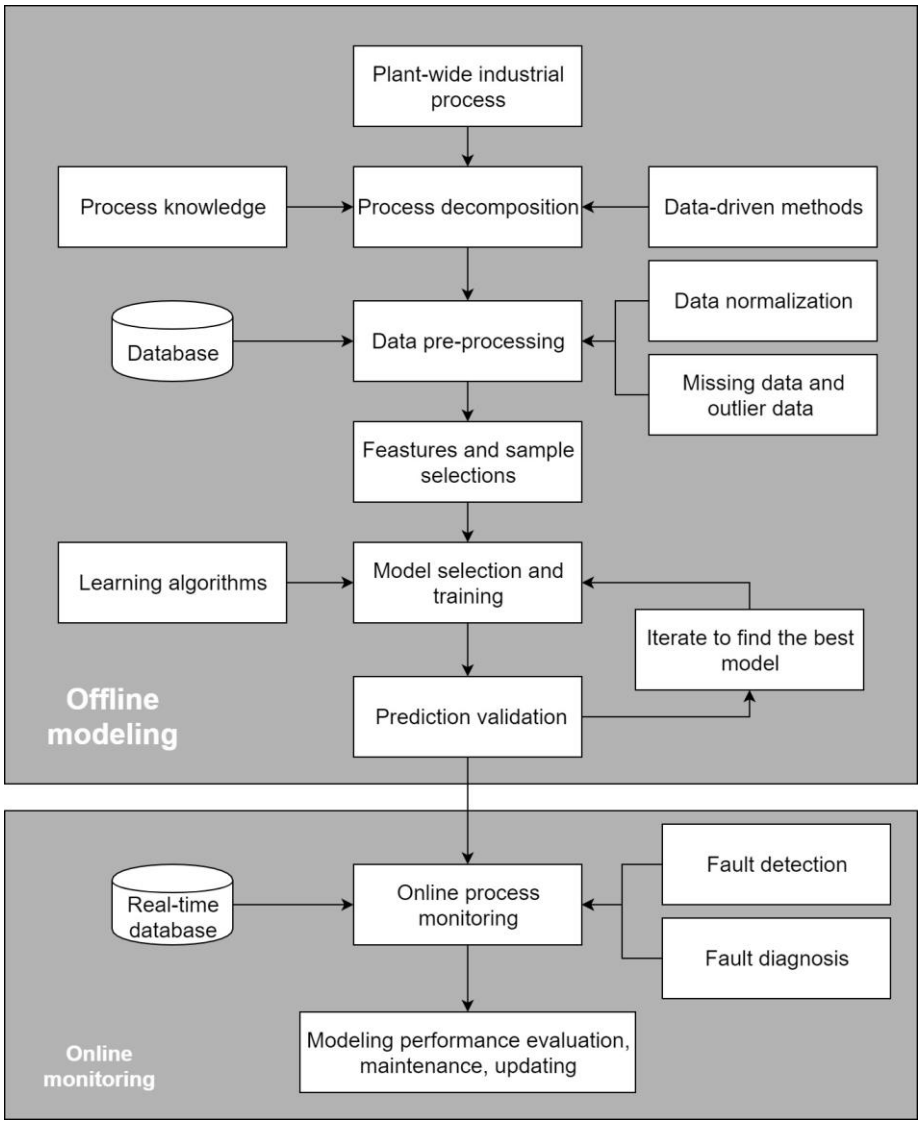

Figure 2. A generic procedure of data-driven modeling and monitoring for plant-wide processes, modified from a framework proposed by Ge (Ge, 2017)

3.2.1 Process decomposition and sub-process

Process decomposition is generally the first step dealing with large scale plant-wide process simulation. This strategy can bring several advantages. Firstly, dividing a complex system into multi-distributed blocks can reduce the computational cost. Secondly, the framework with multi-blocks is more flexible to maintain and to update. Thirdly, the fault tolerance ability will be improved.

The data preprocessing is an essential step in data-driven modeling and the data mining process. Industrial data does sometimes contain errors and incomplete or inconsistent data. Data pre-processing can mitigate such issues and reformat raw data into a logical structure. The general methods utilized in data pre-processing include interpolation, data dimension reduction, normalization and standardization, data features selection, and creation.

Data preprocessing is followed by feature and model selection, where appropriate machine learning algorithms and data model structures are considered. It needs to be mentioned that the model selection is highly related to the data characteristics and relationships among process operational variables (Ge et al., 2017). For example, non-Gaussian data modeling methods should be applied to variables with non-Gaussian distributions; a nonlinear algorithm like artificial neural networks should be conducted if there are nonlinear relations between variables and the desired predictions, or a dynamical learning method should be employed on a time-series problem (Choi et al., 2008).

The next step before online utilization is model validation and performance evaluation. There are some well-defined methods in this process, such as cross-validation, model stability analysis, sensitivity analysis, etc. (Bishop, 2006).

3.2.2 Introduction of generally used data-driven methods

Generally, data-driven methods can be categorized into four groups: supervised learning, unsupervised learning, semi-supervised learning, and reinforcement learning. For industry applications, supervised learning and unsupervised learning are mostly adopted, which account for more than 80 percent usage (Ge et al., 2017). Brief reviews of several representative learning methods are described as follows.

The decision tree is a popular algorithm for supervised learning problems (Hastie et al., 2005). The main idea is to build a binary tree that split its space into two regions. Then this individual branch continues to split into two more regions, and this process repeats until a rule is met. But decision trees are prone to overfitting when a tree is particularly deep.

Random Forests (RF) algorithm was developed by Breiman in 2001 (Breiman, 2001). An RF is a collection of decision trees whose results are aggregated into one result. The overfitting problem can be mitigated by its voting mechanism. RF also improves forecasting accuracy by averaging many noisy but unbiased trees (Zhang and Haghani, 2015).

Gradient Boosting Regression (GBR) is similar to RF. They are both ensemble learning methods and predict by combining the outputs from individual trees. The major difference between GBR and RF is that the probability of selecting an individual sample is not equal in GBR, but in RF, the samples are uniform (Zhang and Haghani, 2015). This random selection helps to make the method more robust than decision trees and less likely to overfit on the training data.

An effective classification and regression method is the K-Nearest Neighbors model (Witten et al., 2016). KNN is one of the oldest and simplest algorithms used in data mining and machine learning. A typical KNN uses Euclidean distances to measure the dissimilarities of input vectors (Weinberger et al., 2006). The decision of a class label to the input pattern is based on its closest neighbors of vectors.

An Artificial Neural Network (ANN) is a flexible and robust mathematical architecture that can identify complex non-linear relations between input and output signals. Inspired by biological nerve systems, the synchronous processing nodes in an ANN are called neurons and are arranged in a computational net (Lippmann, 1987). The parallel neurons connected with activation functions and weights. Once the network is trained, the neural network can be used to calculate the output for any arbitrary set of input data as long as it belongs to the space defined by the training data sets.

3.3 Combination of Fundamental Models and Data-driven Models

It should be noted that data-driven methods have a major limitation that is agnostic to the underlying physics principles. The black-box data-driven models are often highly dependent on the labeled data that they are trained with. The model prediction can be deceptively good on both training and test datasets but is not generalized well outside the available labeled data (Karpatne et al., 2017b). Moreover, the main concern with black-box models is the lack of scientific consistency with respect to the laws of physics. Even though sometimes the predictions have a more accurate performance, data-driven models can not represent their mechanistic understandings of the physical processes.

To combine the advantages of data-driven models and fundamental models, Karpatne (Karpatne et al., 2017b) introduced a framework that uses the knowledge of physics to guide a neural network. Figure 3 illustrates one method that utilizes the physical models on data-driven models. The output of the physics-based model is considered to be a new feature in the data-based model along with the original dataset. Additionally, Karpatne used physics-based loss functions in the learning objective to make the model prediction not only have fewer errors but also be consistent with known physics.

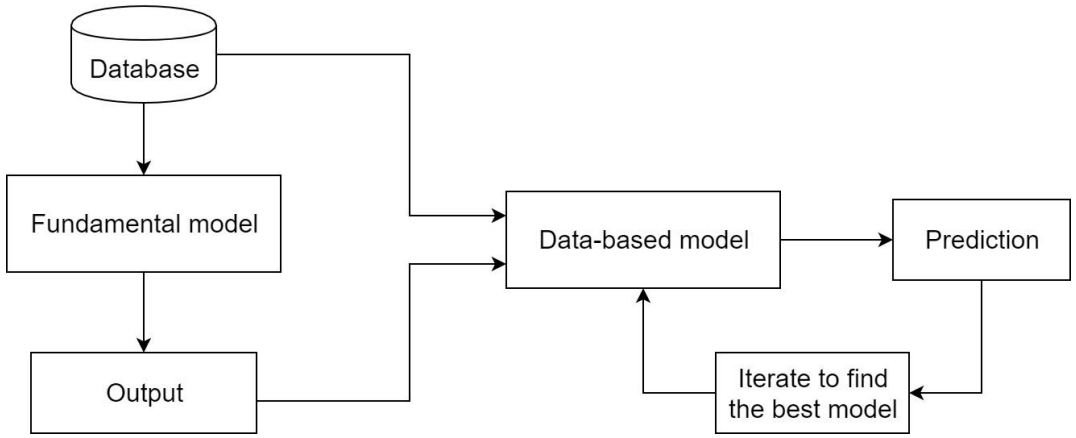

Figure 3. Schematic illustration of a hybrid fundamental-data model. The output of a physics-based model is used as a new feature in a data-based model, modified from Karpatne (Karpatne et al., 2017a).

This kind of hybrid-physics-data structure is studied and applied in many engineering systems. For example, Jia proposed a physics guided recurrent neural network to simulate a lake temperature profiles (Jia et al., 2019), Long applied convolutional Long short-term memory(LSTM) as the backbone to predict the external forces on a dynamic system (Long et al., 2018), and Zhang showed improved performance on simulating a power grid via physics-deep unrolled neural networks (Zhang et al., 2018). Recently investigators have examined the effects of physics understandings on pure data-driven methods. The hybrid-physics-data framework shows better generalizability, and more importantly, it introduces physically meaningful results in comparison to black-box data methods (Karpatne et al., 2017a).

4 METHOD

The aim of this chapter is to:

- Introduce the research methodology used in this thesis.
- Describe the adopted fundamental models of AG/SAG mills and cone crushers.
- Describe the data-driven algorithms for SAG mill power draw prediction.
- Propose a framework for data analysis.

4.1 Fundamental Models

4.1.1 SAG mill model

In both Paper A and Paper B, the proposed dynamic model of an AG/SAG mill includes several interlinked sub-process modules, and each of these modules can be updated individually. As shown in Figure 4 from Paper A, the mill is divided into n sections, where m is the section number， and q is the mass of transported material. All sections have the same length, and each section contains a dataset of particle information at each simulation time step, such as particle size, mass, energy gain, and breakage rate. The dataset is calculated and updated continuously. Each particle is ground into new particles according to the breakage rate and appearance function, and then the probability of moving to the next section is estimated based on the mass transfer coefficient and the slurry flow rate.

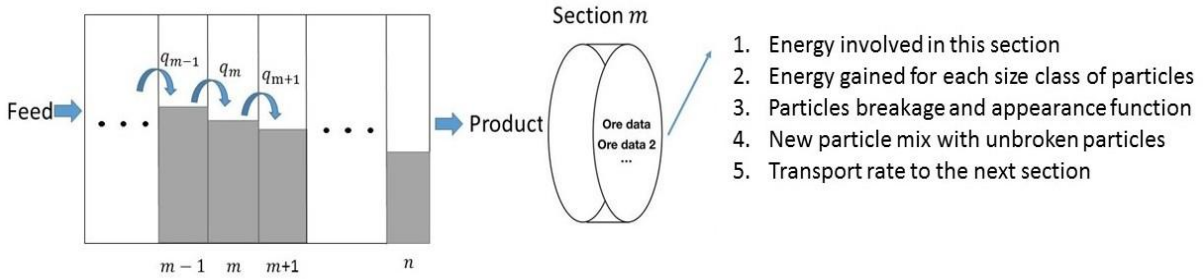

Figure 4. Schematic of data structure in the simulation.

Austin introduced a simple algebraic equation set that describes a time-independent breakage model and treats the mill as a series of fully mixed reactors (Austin and Cho, 2002), as in Equation (4.1).

$$Sel_i = A_1\left(\frac{x_i}{x_0}\right)^{\alpha_1}\left[\frac{1}{1+\left(\frac{x_i}{\mu x_0}\right)^{\Lambda}}\right] + A_2\left(\frac{x_i}{x_0}\right)^{\alpha_2} \tag{4.1}$$

Where Sel_i is the selection function of the size interval indexed by i, x_i is the upper size of the size interval indexed by i, x_0 is a standard size (usually 1 mm). A_1, α_1, μ and Λ is for the nipping breakage of smaller particles by larger grinding media, while A_2, α_2 is for the breakage of large lumps by collision with media and lumps of similar size (self-breakage). The units of A_1 and A_2 are $time^{-1}$. The parameters α_1, α_2, μ, Λ are dimensionless.

The energy applied in each section can be estimated as:

$$E_i^m = \frac{E_{tot}}{n\cdot\left(\sum_{i=1}^{j} m_i + m_{ball}\right)} \tag{4.2}$$

In Equation (4.2), there are n equally long sections and E_i^m is the mean energy ($[kW/t]$) for particle size class i in section m. m_i is particle mass of size class i and m_{ball} is the steel ball mass, and E_{tot} is the total net energy applied on the mill charge.

In work from Paper A and Paper B, we use the standard Broadbent-Calcott model (Whiten, 1974) for the appearance function instead of the JKMRC t_{10} model, as expressed in Equation (3.5) and Equation (3.6). The standard appearance function covers a broader size range and is independent of ore type. This standard appearance function is for validating the proposed hypotheses in a general way. The JKMRC model and laboratory test are conducted on the actual ore, and it can provide more accurate information to a specific plant.

The transport function plays a very important role in the dynamic mill modeling. It has a significant influence on the particle size distribution, mill load, throughput, resident time, and other parameters (Yu et al., 2014). In this work, the mill is modeled as a combination of a series of sections. Particles in each section are considered to be perfectly mixed. The diffusion relations for each ore size class are described in Equation (4.3).

$$q_i = -D_i \cdot \frac{d\rho_i}{dx} \tag{4.3}$$

Where i indicates the i th size class of particles, q is the mass flux through the controlled area, D_i is the mass transfer coefficient and $d\rho/dx$ is slurry density changing along the mill sections. The transfer coefficient needs to be tested and updated from pilot or plant data.

The discharge function for each particle size class in AG/SAG mills can be expressed as the maximum discharge rate (D_{max}) times the classification function, see Equation (4.4). The classification function is characterized into three zones (Kojovic et al., 2012) using the size of slurry (particles smaller than this size behaves like liquid), size of grate aperture, and pebble port size.

$$d_i = D_{max} \cdot c_i \tag{4.4}$$

Where d_i is the discharge rate of size class i, c_i is the classification function for size class i.

Valery and Morrell (Napier-Munn et al., 1996) developed a conceptual dynamic model for AG/SAG mills to provide an accurate dynamic response such as power draw, mill charge level, product size distribution feed hardness, etc. In Paper A and Paper B, the dynamic equations are updated based on Valery and Morrell's equation, see Equation (3.3), the particle population model for each section in a mill is described in Equation (4.5). In this dynamic equation, the material change in each section is calculated individually:

$$\frac{ds_i(t)}{dt} = q_i^{in} - q_i^{out} + \sum_{j=1}^{i} r_j s_j a_{ij} - r_i s_i \tag{4.5}$$

Where s_i is section content of size class i at time t, q_i^{in} is particles transported from the previous section of size class i, q_i^{out} is particles transported to the next section of size class i, r_i is particles breakage rate of size class i, a_{ij} is appearance function, size class i break from size class j. At the first section, q_i^{in} is feed particles of size class i, and at the last section, q_i^{out} is discharged particles of size class i.

The dynamic framework presented in Paper A and Paper B treats a mill as a series of perfectly mixed sections along with a breakage/appearance function and a mass transfer function. The method applies basic calculation rules and avoids utilizing too many empirical relations. This means that at each simulated time step, the fresh feed, product, and mill operating parameters are considered. The status of all particles is calculated regarding breakage probability, motion behavior, position in the mill, discharge chance, and so on. If the system reaches stable operation within a certain period, it is considered a steady-state. This model is supposed to be based on the real plant data and back-calculate the sub-process functions used before, which consequently leads to an extensive application and more accurate predictions.

4.1.2 Cone crusher model and other equipment

In Paper B, the dynamic behavior of the entire system, including the SAG mill and cone crusher operating in closed circuit, is examined. Therefore, in addition to the SAG mill model, the dynamic simulation of cone crushers, conveyors, bins, and screens are also included.

Asbjörnsson (Asbjörnsson, 2015) studied the dynamic crushing plant behavior and discussed the machinery bottlenecks that affect throughput. Here, dynamic models similar to those presented by Asbjörnsson were used to model conveyors and screens. A pure time delay is used for the conveyor model regarding its length and speed, as seen in Equation (4.6). Also, the screens are modeled with a constant time delay, which depends on the screen size. The large surge bin for material storage is assumed to be perfectly mixed, and the level in the bin is a function of mass flow and the bin dimensions.

$$\chi(t) = u\left(t - t_{delay}\right) \tag{4.6}$$

A small bin is modeled for the cone crusher chamber, where the particles are perfectly mixed. The product particle size distribution of the cone crusher is shown in Figure 5 from Paper B. The eccentric speed settings in Figure 5 are 280, 360, and 440 rpm. It can be seen from the plot that the CSS and eccentric speed of a cone crusher can affect the final PSD significantly. A change in CSS of the crusher moves the product PSD horizontally while eccentric speed turns the curve around a pivot point (Hulthén, 2010). Furthermore, the crusher capacity is also a function of CSS and eccentric speed, as shown in Figure 6 from Paper B. With a given CSS, the capacity decreases for a higher eccentric speed.

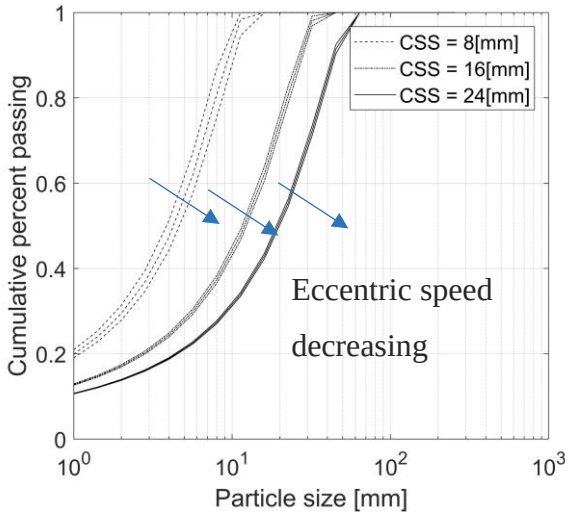

Figure 5. Product PSD of different cone crusher settings. Data from Evertsson (Evertsson, 2000), tested on a Svedala Hydrocone cone crusher.

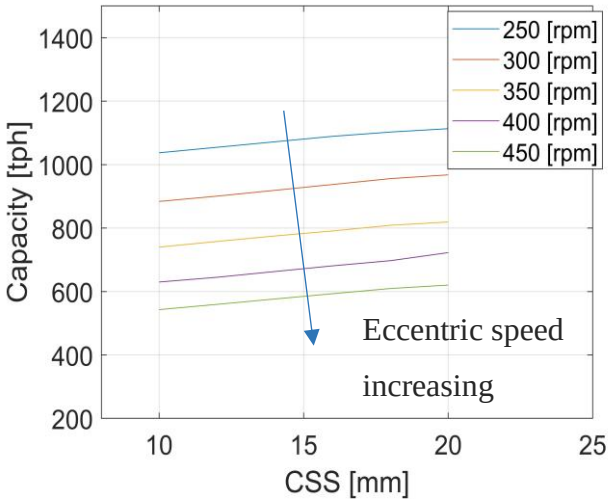

Figure 6. The capacity of cone crushers with different settings. Data from Lindqvist (Lindqvist and Evertsson, 2004), tested on an FLS Raptor 900 cone crusher.

4.2 SAG Power Model with Data-driven Methods

Two data-driven methods are presented in Paper C, where a SAG power prediction and a two-minute power forecasting are performed. The forecasting model uses modified Recurrent Neural Networks (RNN). Recurrent neural networks are developed to recognize patterns in sequences of data, such as text, the spoken word, numerical time series data, and the stock

market. But standard RNNs fail to learn long time lags between relevant input events and target output signals (Gers et al., 1999). Later, a special recurrent neural network called Long Short-Term Memory (LSTM) was developed by German researchers Sepp Hochreiter and Juergen (Hochreiter and Schmidhuber, 1997). LSTM was designed to overcome the problems of vanishing gradient and store information for long periods to solve complex long-time lag issues (Marino et al., 2016). Figure 7 illustrates a single LSTM cell.

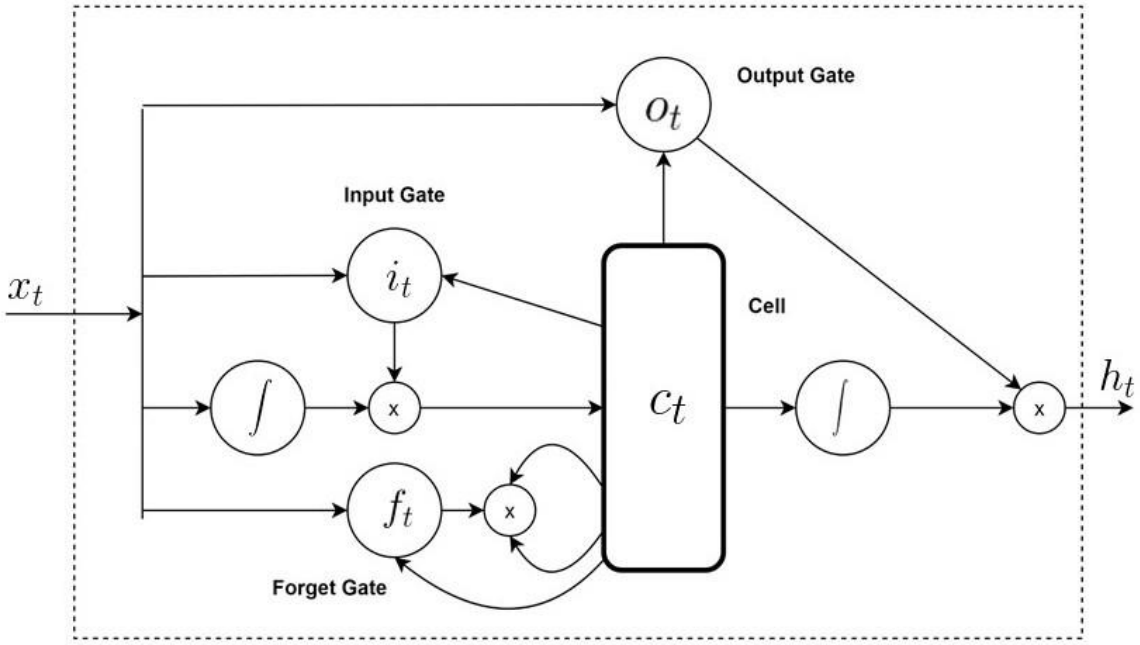

Figure 7. Long Short-term Memory Cell structure.

The key equations of an LSTM network are shown through Equation (4.7) (Graves et al., 2013):

$$\begin{aligned} i_t &= sigm\left(W_{xi}x_t + W_{hi}h_{t-1} + W_{ci}c_{t-1} + b_i\right) \\ f_t &= sigm\left(W_{xf}x_t + W_{hf}h_{t-1} + W_{cf}c_{t-1} + b_f\right) \\ c_t &= tanh\left(W_{xc}x_t + W_{hc}h_{t-1} + b_c\right) \\ o_t &= sigm\left(W_{xo}x_t + W_{ho}h_{t-1} + W_{co}c_t + b_o\right) \\ h_t &= o_t \tanh\left(c_t\right) \end{aligned} \tag{4.7}$$

In the equations, i_t denotes the input gate, f_t denotes the forget gate and o_t is the output gate. x_t is the input signal at time step t and h_t is the cell output. W is the weight matrix, $sigm$ is the logistic sigmoid function and $tanh$ is the hyperbolic tangent function.

Two different data-driven models are introduced for different purposes. The first method is trained with data points at a certain time step to estimate the SAG power draw at the same time step. This data-driven model is widely used for complex non-linear input and output relations. Four algorithms were adopted from the basic statistical method KNN to the advanced ensemble

method RF and GBR. A combination of these four methods, weighted by their errors was then performed, see Equation (4.8) and (4.9). Generally, the integrated result will show better accuracy than in the individual results.

$$w_i \leftarrow \frac{1}{MSE\left(P_i\right)} \tag{4.8}$$

$$E = W \cdot X \tag{4.9}$$

Where w_i is the weight, W is the weight vector, and E is the combined predictor.

The second method in Paper C is a forecasting model, implementing historical and present data points to make the SAG power draw forecasting. The algorithms structure in this method is a combination of Convolution Neural Networks (CNN) and LSTM. The prediction model is more in line with our expectations of the SAG dynamic model and has better application potential, which can be used for advanced process control.

The sliding window technique can reframe the original dataset for the forecasting model, in which a fixed-length window slides along the dataset and saves the data within as the training/testing input. Figure 8 from Paper C demonstrates the sketch of data structures of two proposed methods. The left data structure is for the SAG mill power prediction with the same time step. The right one presents the reframed data structure of the forecasting model. The time-series forecasting model data size increases dramatically and thus requires much larger computational power, though using the same raw dataset.

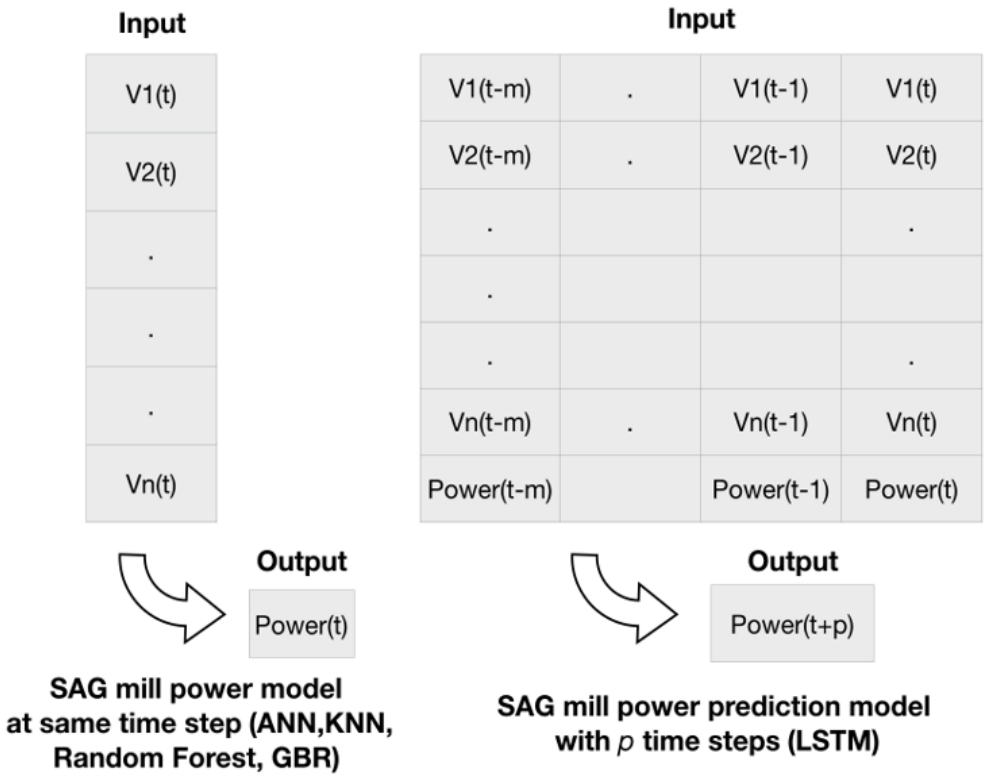

Figure 8. A sketch of training data structures for predicting and forecasting data-driven models.

4.3 Data Mining and Data Analysis

A framework of data analysis that can isolate the impact of a specific variable on the target is introduced in Paper D. The method allows one to extract information by investigating historical data and therefore evaluate patterns of various operating settings on processing performance. Suriadi (Suriadi et al., 2018) introduces an Integrated Analysis Method (IAM) that combines and studies both rock properties and operational data. With this framework, a wide range of analysis tools can be included and implemented. Modified from IAM, the procedure of isolating certain variables is illustrated in Figure 9. The steps of conducting an analysis are listed below:

- Firstly, the preprocessing should be applied to the original dataset to remove the outliers, missing data, and noise.
- Secondly, data patterns are examined by clustering analysis. Different clusters through the dataset may be identified, which correspond to various operating modes of the process (Ge et al., 2017). The clustering methods are designed to discover groups among n individuals described by Q variables (Maugis et al., 2009). Generally, there are two main categories of clustering methods. The first one measures the distances between each data point, like K-means and tree structures. The second method considers a certain model for clusters and tries to fit the data points with this model, like Gaussian mixture distributions.
- The next step is to select the key variables and then cluster them into new labels. Once the clusters are determined, new columns of labels can be added to the dataset based on clustered groups. In this case, the studied critical variable is the pebble crusher utilization based on crusher power and pebble specific energy. The target variable is the fresh feed rate to the SAG circuit.
- The last step is to establish the mapping between clustering variables (crusher utilization) and target performance variables (fresh feed rate). Statistical differences should be visualized in this part, such as showing that one cluster has higher tonnage or some variables are more sensitive to the rock feed size.
- Eventually, one can draw conclusions on some essential operating conditions that are correlated to the target process performances.

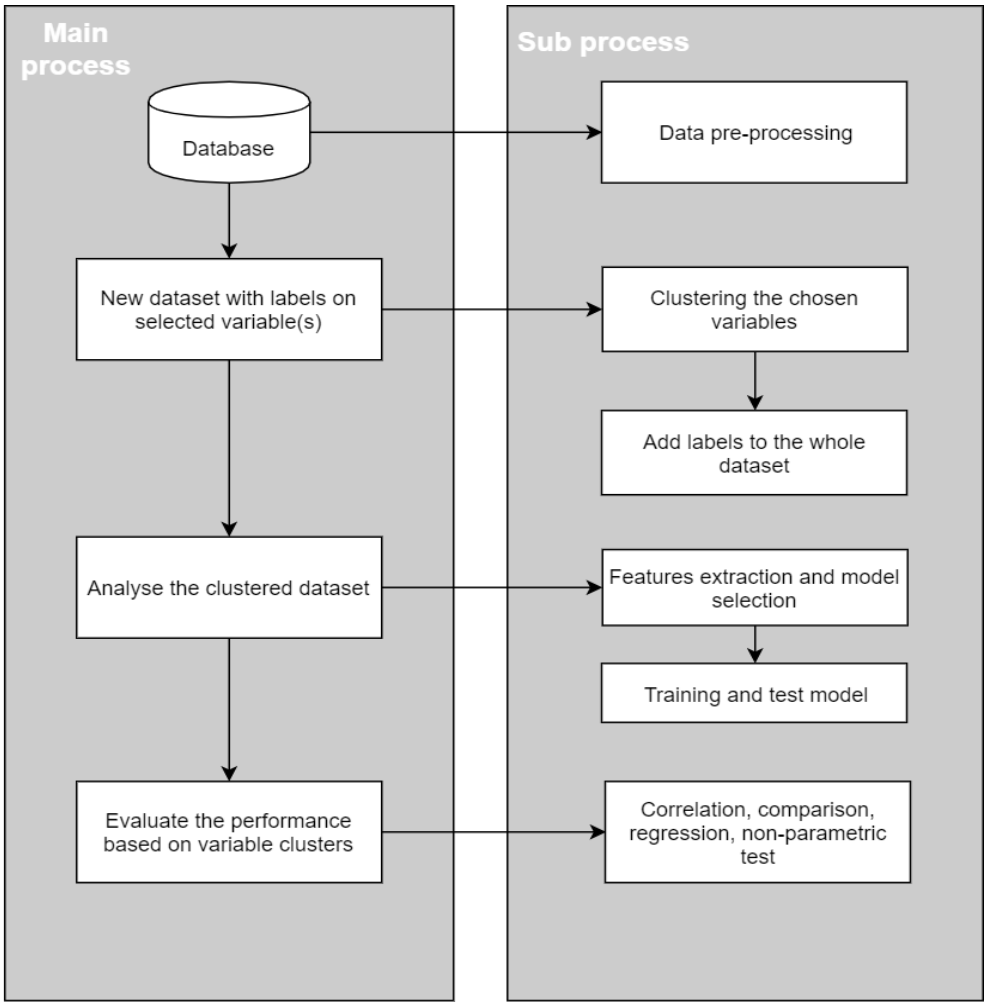

Figure 9. A generic procedure of isolating a certain variable.

5 RESULTS

The aim of this chapter is to:

- Present the simulation results.

5.1 SAG Mill Dynamic Modeling

In Paper A and Paper B, dynamic models for AG/SAG mills were presented. The models have a similar structure and share fundamental ideas. The mill model was divided into discrete sub-processes of physical interactions that occur within the mill. Particle breakage, transportation, and discharge behavior were calculated and updated over time in the simulation.

The single mill dynamic model was evaluated and compared with Yu's work (Yu et al., 2014). A similar feed rate to the mill was used to validate the dynamic response of the mill. As shown in Figure 10, the mill is initially empty, and a constant feed rate starts from 0 to 600 tph at t=100 min, it decreases to 480 tph at t=400 min, and then it increases again to 780 tph at t=700 min. The flow rate of the mill product also changes accordingly as a response to the feed changes.

The mill begins to discharge material at time t=120 min, and it takes about 1.5 hours for the mill to reach a steady state. The time delay between the mill feed and the product is mainly explained by two aspects. Firstly, the material in the mill needs to be ground and transported to the other end before it can be discharged. Secondly, because of the design of the grate, the ore in the mill must have a sufficient volume to reach the apertures and get discharged. Figure 11 shows the product PSD of each section. The mill was divided into four sections. The particles in the mill were progressively ground as predicted when they moved along the milling chamber.

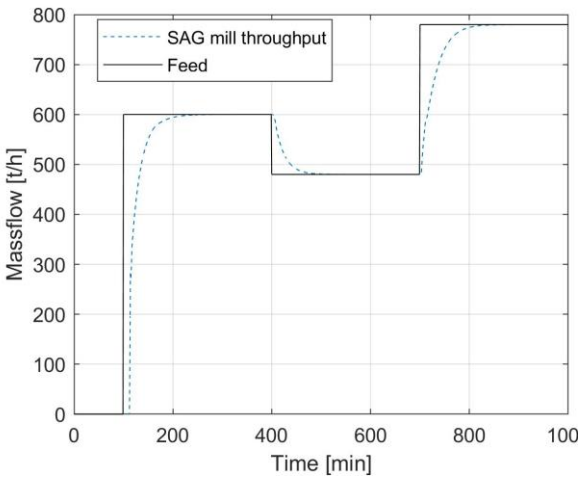

Figure 10. Dynamic response of the mill with a different feed rate.

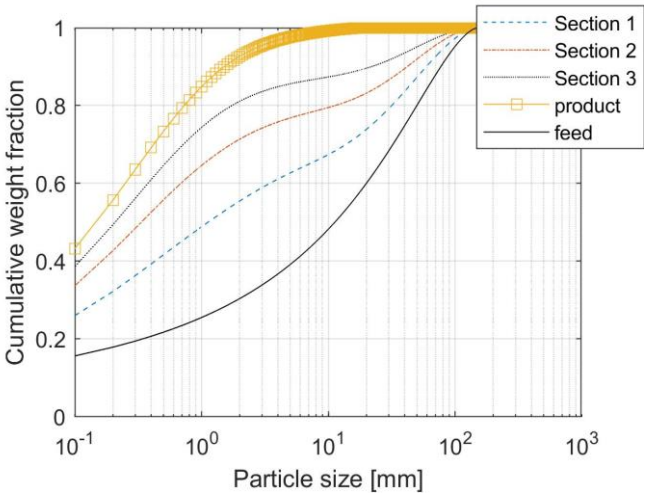

Figure 11. The particle size distribution of different sections in the mill at t = 1000.

5.2 SAG Mill Power Draw Prediction Modeling

In Paper C, the focus is mainly on the power model of SAG mills based on data-driven methods. The original dataset consists of measurements for more than 29,000 data points in the SAG mill-pebble crusher circuit at the Copper Mountain mine. There are 24 variables in the collected operating data, including SAG power, SAG feed size, SAG main bearing pressure, fresh water added to the mill, crusher power, recycling load, and crusher product size, etc.

Two different methods were presented. The first method employed a SAG mill power prediction model using artificial neural networks, K-nearest neighbors, random forests, gradient boosting regression, and their weighted prediction errors to formulate an ensemble model. Thus, this model provides a soft measurement of mill power draw with other variables.

The results for individual models and the ensemble model are shown in Figure 12. The mean squared error (MSEs) were carried out as listed in Table 1 to give the prediction accuracy. The RF and GBR are inherently advanced ensemble algorithms, and both algorithms showed fewer errors compared to ANN and KNN, while the combination of the four models weighted by their MSEs gave an improved result. In Figure 12 from Paper C, when the mill power dropped dramatically at 600 mins, all model results showed some deviations to the real value.

Table 1. Comparison of test errors (MSEs) for proposed individual methods.

	ANN	KNN	Random Forest	Gradient Boosting	Ensemble
Test error (MSE)	0.0077	0.0058	0.0052	0.0046	0.0044

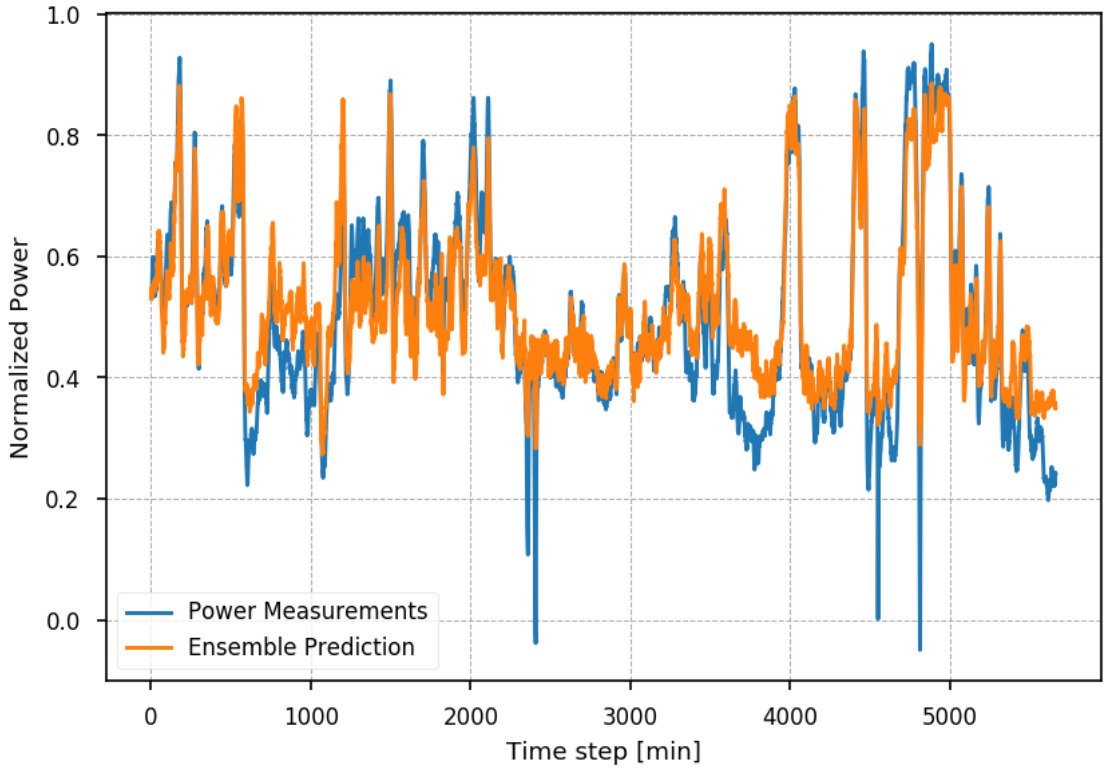

Figure 12. SAG mill power prediction with weighted results from individual predictors

The explanations of the deviations could be that some important features were not included in the training dataset. When these features changed, the proposed models could not bridge the gap between predicted and real power due to the missing information. Though there existed some errors when the mill power decreased dramatically, the overall trends still fitted the predictions well. The deviations were expected to be further reduced by introducing diverse datasets, more training iterations, model tuning, and proper data pre-processing.

The second method considered the SAG mill power draw to be a time series problem. The original dataset was reformatted by a sliding window and trained with an LSTM algorithm. This LSTM forecasting method took twenty-minute historical data and predicted a two-minute mill power draw.

This forecasting algorithm included one Convolutional Neural Network (CNN) layer and two LSTM layers connected by a Fully Connected (FC) layer, see Figure 13. The training data first passed through a CNN layer, which preliminarily analyzed the characteristics of multiple consecutive time data and their trends. Then the LSTM layers were implemented to further extract the patterns from different periods. The model performed a promising SAG power forecasting shown in Figure 12. The FC layers in between the CNN and the LSTM reframed the data structure to a particular format without changing any information. In addition, the dropout layers were introduced, and they deleted some information randomly between two connected layers in order to avoid the model over-fitting.

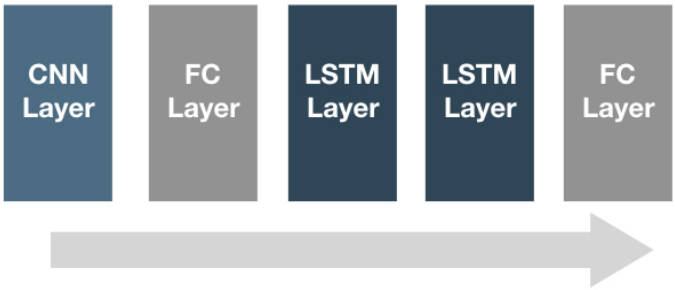

Figure 13. Sketch of the forecasting model structure with CNN layers and LSTM layers.

A sliding window technique was adopted to reformat the input data. A large window width can capture more continuous-time information, though the amount of computation will increase significantly. Meanwhile, a small window width can be too narrow to contain enough patterns. In this study, a window width of 20 minutes and a forecasting step size of 2 minutes were chosen, which means the algorithm made a 2-minute SAG mill power draw forecasting by feeding with the 20 minutes of historical data. Throughout sliding window processing, the input data held both time dimension information and feature dimension information. It can be seen in Figure 14, that the proposed method is able to perform accurate 2-minute forecasting on SAG mill power draw.

The data-driven methods presented in Paper C are flexible, easy to employ with suitable datasets, and show a great advantage in optimizing SAG power draw for rapidly changing conditions. Moreover, the forecasting method provided a significant potential in fault detection and predictive control of the grinding processes.

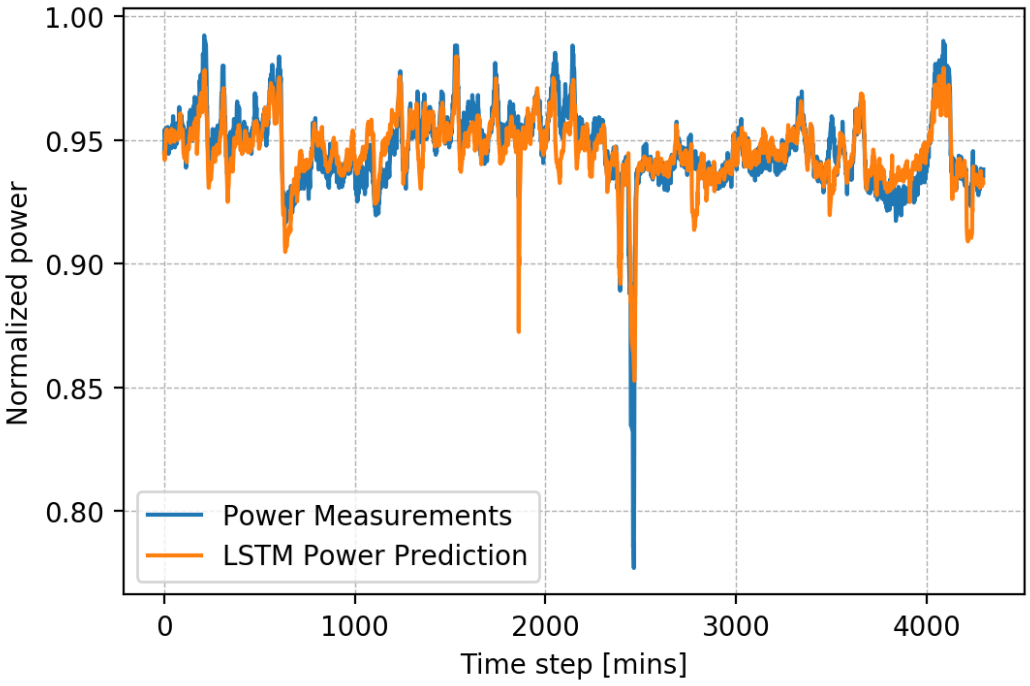

Figure 14. 2-minute forecasting model for SAG mill power with 20 minutes of historical data.

5.3 The Impact of Recycling Load on a SAG Mill Circuit

In Paper D, the main purpose was to isolate and systematically investigate the impact of the recycling load and pebble crusher operational settings on the total grinding circuit performance. The influencing variables have been selected to be the crusher power and pebble specific power. The fresh feed rate has been selected to be the circuit performance variable.

It is shown in Figure 15 that the pebble crusher power and pebble specific energy have different distribution patterns. The variables represent 'how much work' the crusher has done on the recycling load. Since the data points are very close to each other and have some distribution behaviors, the Gaussian mixture method was used, and group numbers were set to be 4. It can be seen from Figure 16 that these 4 clusters are with zero crusher specific energy (SE zero), low crusher specific energy (SE L), middle crusher specific energy (SE M), and high crusher specific energy (SE H), respectively.

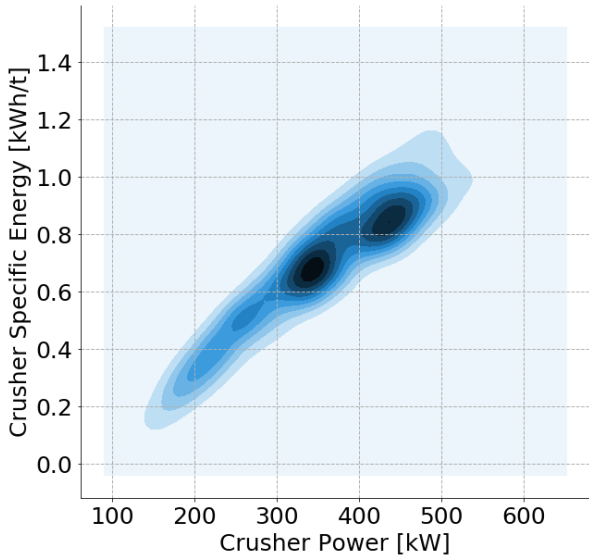

Figure 15. Kernel density estimation plot of the pebble crusher power and pebble specific energy.

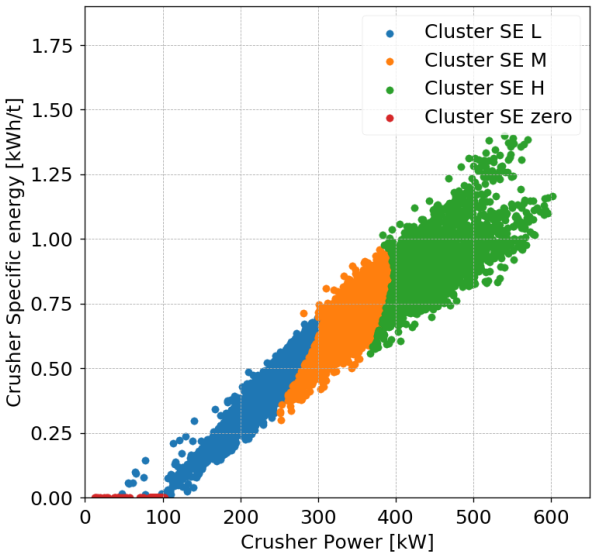

Figure 16. Clusters of recycling load based on crusher power and pebble specific energy.

The next step of data analysis is to identify the key performance variable, which is the SAG mill fresh feed rate. The change point analysis (CPA) was implemented to identify patterns from the time-series dataset. CPA is a powerful tool for determining whether a change has actually occurred or not (Taylor, 2000). This analysis was conducted by Ruptures package in Python (Truong et al., 2018) and found 66 changes over the whole dataset, see Figure 17. Then these periods were separated based on their averages, which are 1619 tph, 1720 tph, and 1821 tph, respectively. The corresponding rows in the dataset were then labeled according to the fresh feed rate. It needs to be noted that a data point with a low SAG mill feed rate (such as 1600 tph) can still be labeled with a 'high feed rate' as long as the period the data point belongs to has a high average value and vice versa.

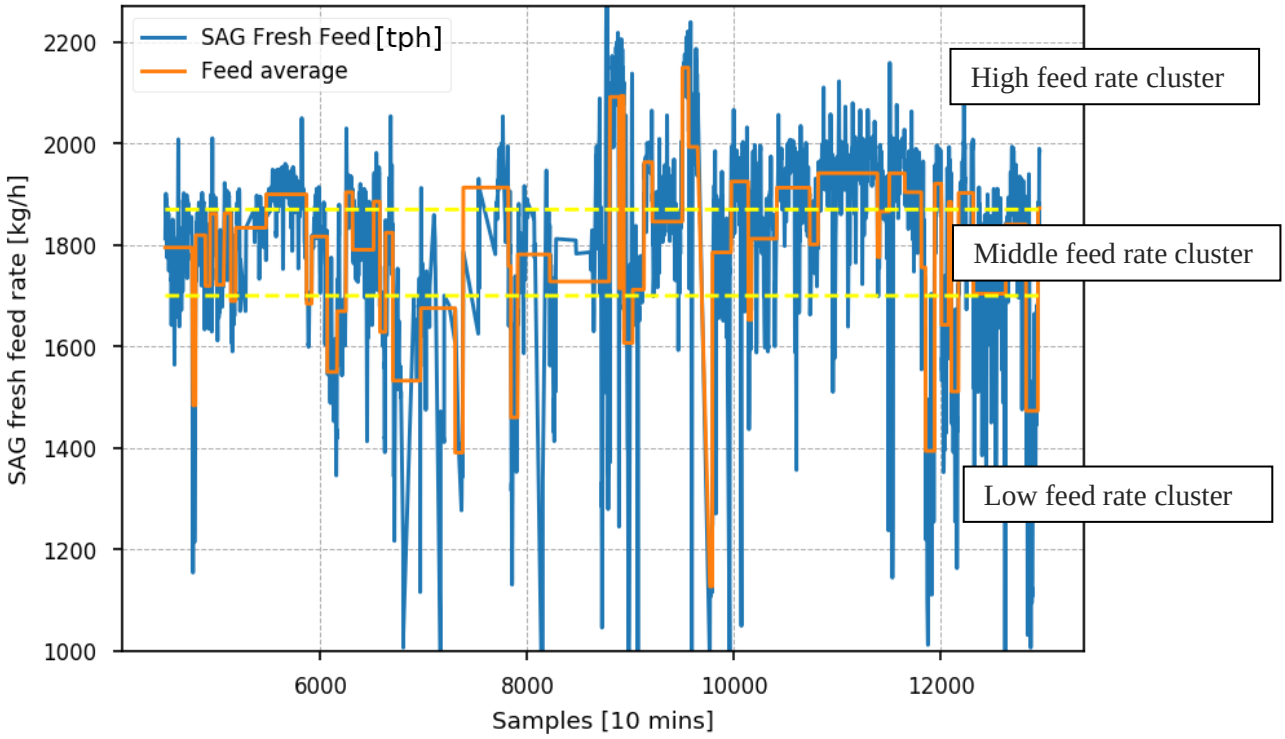

Figure 17. Change points of fresh feed rate. It is categorized into three classes based on their average value in each period.

In the final step, the impact of the key variables on circuit performance was investigated. From Figure 18 (a) to (d), circuit performance variables such as SAG power, SAG feed rate, and SAG specific energy are compared with their crusher cluster labels.

The SAG mill specific energy was calculated from SAG power draw and fresh feed rate, as seen in Figure 18 (a). Data points with SE H has an average SAG specific energy of 6.9 kWh/t compared to 7.5 kWh/t with SE L, corresponding 8% decrease in specific energy.

In Figure 18 (b), the fresh feed size slightly differs from these three clusters from 49.1 to 51.0 mm, and it indicates that all clusters contain data points with similar feed rock size. Therefore, the circuit performance differences are not likely caused by feed size varieties. Moreover, the original dataset was from Copper Mountain, where a pre-crusher has been installed to feed the SAG circuit. The size distribution of fresh feed to the SAG mill was considered consistent.

Figure 18 (c) and Figure 18 (d) are SAG fresh feed rate and SAG total tonnage (fresh feed and recycling feed), respectively. Both results show clear trends that data points with SE H have higher values than those with SE L. The average fresh feed rate with low crusher utilization is 1715 tph, while the fresh feed rate increases to be 1850 tph. The total tonnage of the SAG mill increases from 1980 tph to 2266 tph with a SE H label.

In brief, the visualized results with crusher power/specific energy clusters show strong correlations between pebble crusher operational settings and circuit performance variables.

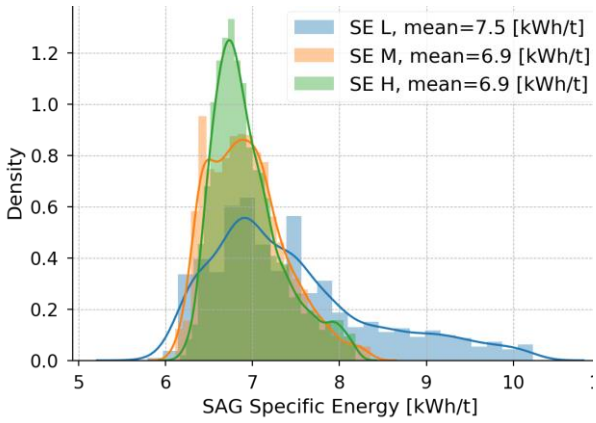

Figure 18 (a). The SAG mill specific energy distribution.

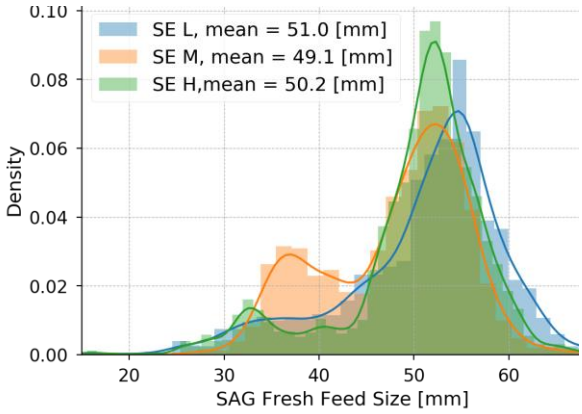

Figure 18 (b). The SAG mill feed size f_{80} distribution.

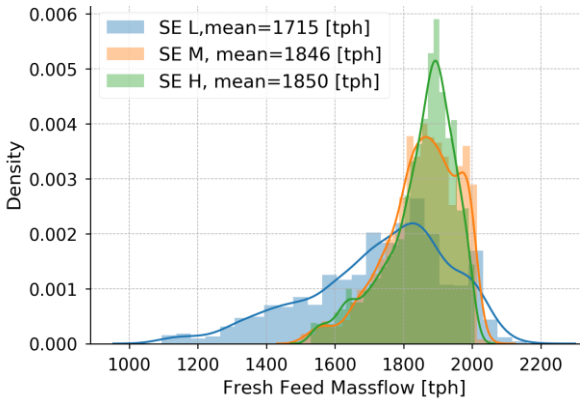

Figure 18 (c). The SAG mill fresh feed rate distribution.

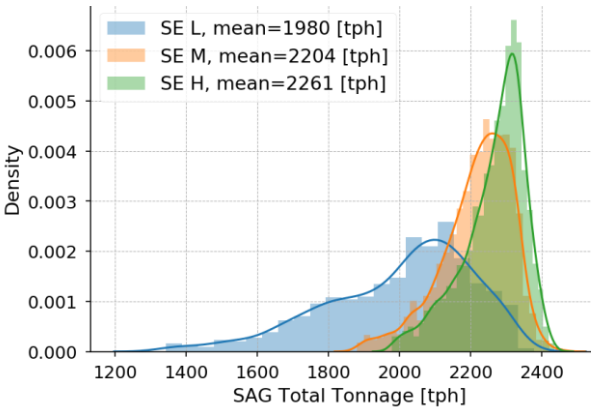

Figure 18 (d). The SAG mill total tonnage distribution.

To further validate the hypothesis that fully utilizing the pebble crusher leads to a higher circuit tonnage, data points with feed rate labels are presented in Table 2 and Figure 19. The mean values of recycling pebble flow rate and pebble size in Table 2 show that the recycling load is very similar in all cases. Furthermore, the fresh rock feed size to the SAG mill shows no significant difference either.

The statistical results indicate that the crusher behavior is not mainly driven by the SAG mill, though a higher SAG tonnage gives a slightly higher pebble flow rate. By contrast, when the pebble crusher maximized its power utilization to break critical size rocks into finer particles as presented by the pebble specific energy in Table 2, the circuit throughput was boosted.

Table 2. Comparison of circuit variable average values based on feed rate labels

Variables	Feed rate low	Feed rate mid	Feed rate high
SAG fresh feed size [mm]	51.2	50.4	50.6
Pebble size [mm]	38.2	37.1	37.3
Pebble flow rate [tph]	292	310	307
Pebble specific energy [kWh/t]	0.55	0.66	0.78

A summary of the identified categories is shown in Figure 19. In the low feed rate period (mean value 1619 tph), 794 data points belong to 'low utilization of crusher', while the high feed rate period (mean value 1821 tph) contains 1054 data points with 'high utilization of crusher' labels. As each crusher cluster has similar rock feed size, the distribution difference is likely caused by the crusher operational setting differences. Therefore, it is reasonable to conclude that higher utilization of pebble crusher leads to a higher circuit throughput.

The framework presented in this paper focused on data analysis and correlations between some critical inputs to the performance outputs. This data-driven technique is flexible to extract and gives insights about the information from rock characteristics, machine operational settings, to circuit throughput, and it can help find correlation between variables in a given process.

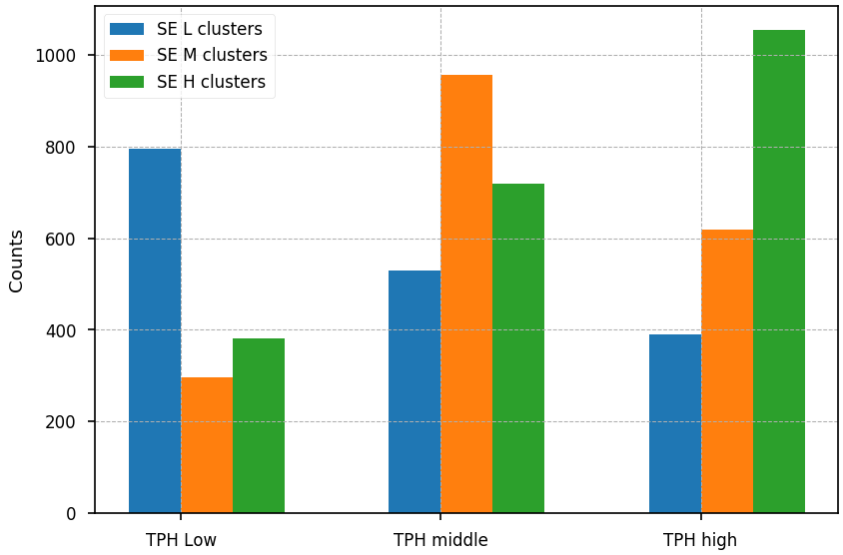

Figure 19. The correlations between crusher clusters and SAG mill fresh feed rate clusters.

5.4 SAG Mill with Pebble Crusher Circuit Dynamic Modeling

The dynamic modeling of the grinding circuit was discussed throughout Paper B. Dynamic fundamental models were implemented and combined on SAG mills, cone crushers, screens, and conveyor belts. Two numerical examples have been demonstrated in the paper. The first

simulation was a typical SAG-cone crusher circuit. It tested the dynamic response of the AG/SAG model with feed size data, flow rate, in mill transportation, in mill particle size distribution and interactions with a cone crusher, and a screen. The second scenario considered a more complex situation where two identical SAG mills and two cone crushers were included. The recycling load was more than one cone crusher could handle, so the second cone crusher was switched on and off to keep the surge bin storage from flowing over.

5.4.1 A typical AG/SAG-pebble crusher circuit

A simulation of a typical SAG-pebble crusher circuit was made to validate the hypothesis as well as to illustrate the capability of the dynamic model. The computational process was simulated with Matlab/Simulink, as seen in Figure 20 from Paper B. This plant had zero fresh feed at the beginning. Fresh feed to the plant started from t=100 min to t=800 min with a flow rate of 480 tph and drops to 340 tph after t=800 min.

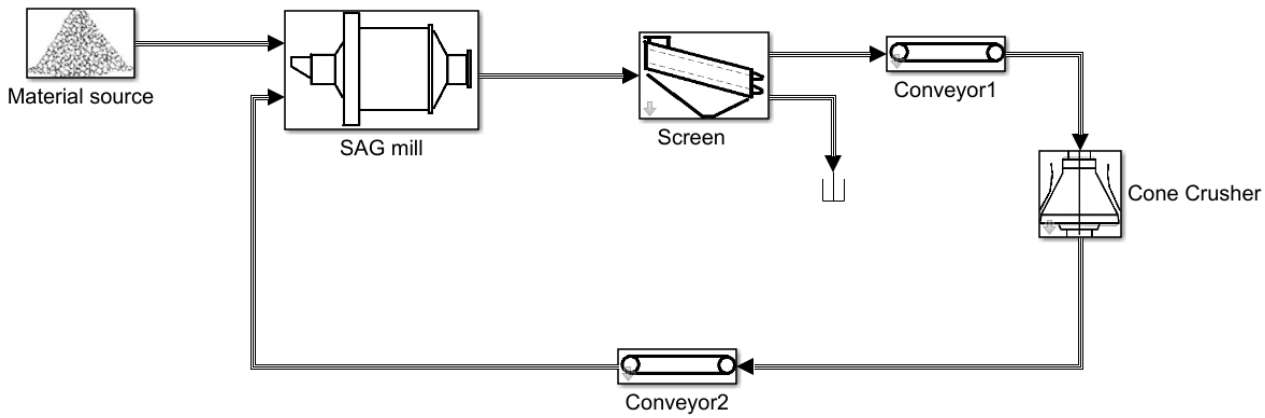

Figure 20. Flowsheet of the simulation scenario 1

Figure 21 shows the feed rate to the plant with 5% noise and its dynamic responses to various cone crusher settings. The SAG product time delay in the top plot is due to the dead slurry pool and particle transport within the chamber. It can be seen from the second plot in Figure 21 that the recycling loads are about 15% to 20% of the feed rate, among which 'no cone crusher' shows the highest recycling load and crusher with 'CSS=10 mm, speed=400 rpm' gives the lowest. The third plot shows the plant throughput. It shows a different response time to become a steady state.

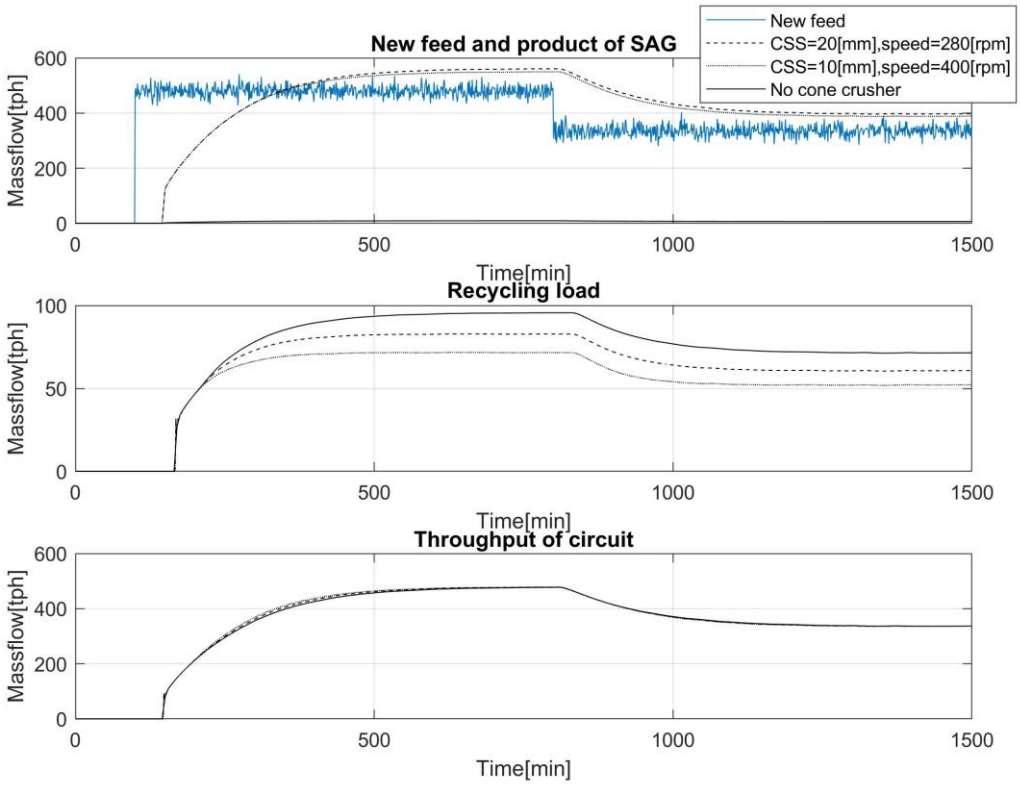

Figure 21. Simulation results from simulating scenario 1

Figure 22 and Figure 23 shows the particle size distributions inside the SAG-mill at different time steps with cone crusher settings CSS=20 mm, speed=280 rpm. In this simulation, the SAG-mill was divided into 10 sections. Figure 22 shows the PSD in section 1, section 4, section 7, and product. The particles in the mill are progressively ground. As expected, PSD gets finer as the material moves along the mill. At non-steady state, t=150 min, the particles in the chamber are coarser than steady-state at t=1500 min, see Figure 23. This phenomenon is due to the SAG mill and plant dynamic response. Firstly, the ores needed more time to be ground. Secondly, the recycling load was relatively small at the beginning, so less fine particles were recycled to the SAG mill. The PSD then continuously got finer until the steady-state was reached. On the other hand, if we look closely and compare PSD at t= 820 and t=1500, the PSD at t=820 is a little bit finer. This was because the new feed to the SAG dropped, but the recycling load was still high.

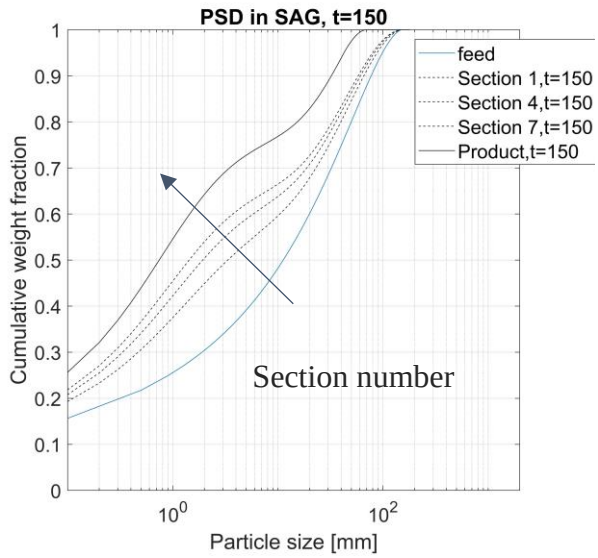

Figure 22. PSD in SAG mill, simulation time at 150 min

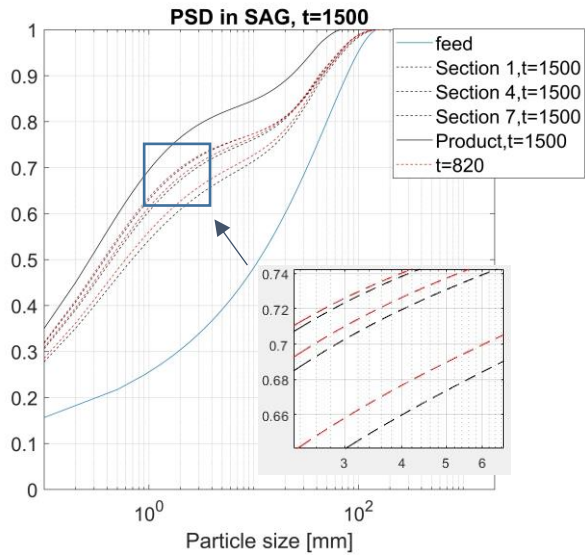

Figure 23. PSD in SAG mill, simulation time at 1500 min

5.4.2 Responses of a double SAG mill circuit with two cone crushers

In a second scenario, a more complex circuit was modeled. The circuit shown in Figure 24, has two identical SAG mills in parallel and two pebble crushers after the screens and a surge bin for the critical size particles. In this scenario, one cone crusher alone was not capable of handling all the recycling products. A second cone crusher needed to be switched on and off to keep the level in the surge bin below 100%. The purpose of this simulation was to study how the settings of the cone crushers can affect the circuit dynamics and the final product PSD.

The assumptions for this scenario are listed below.

- The capacity of all components will stay the same, regardless of wear.
- Cone crusher 1 always runs at 100% capacity, and when the level in the bin reaches 300 tonnes, the second cone crusher will be switched on, which also runs at 100% load.
- Bin 1 and Bin 2 work as perfect mixing surge bins. The full load for Bin 1 is up to 300 tonnes, and Bin 2 storage capacity is neglected so it works like a perfect mixer.
- The ideal screens and splitters are used to separate the stream so as to keep the recycling load the same for both mills.

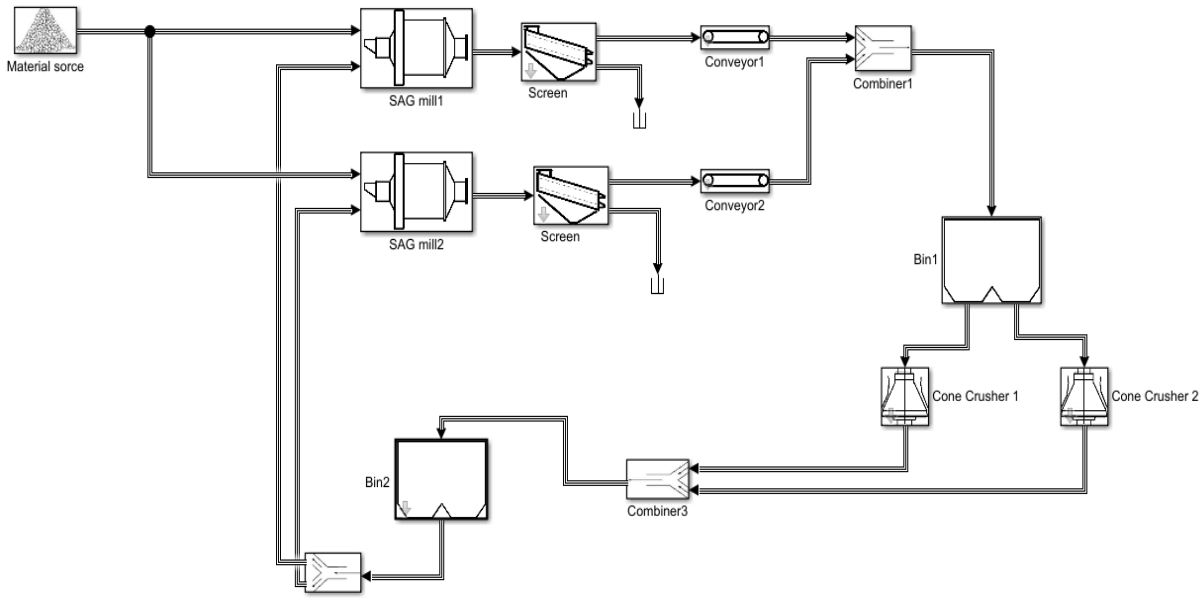

Figure 24. Flowsheet of the simulation of scenario 2

The first graph in Figure 25 shows the new feed rate to the plant and the throughput of one of the SAG mills. In this circuit, two SAG mills have the same throughput, feed rate, and recycling load. Below are all the simulation results from SAG mill 1. The first graph shows that the throughput of the SAG mills is affected by the pebble crusher settings. A cone crusher with settings like CSS = 28 mm and speed = 280 rpm gives a coarser product than a cone crusher with smaller CSS and higher eccentric speed. The crusher's capacity with a larger CSS and lower speed is higher than with a small CSS and high speed. The second graph in Figure 25 shows the recycling load. The second cone crusher is switched on and off according to the mass level in bin1, as seen in the third plot. The last two graphs show the throughput of the SAG mill and the charge in the chamber. The mill charge is directly related to the power draw of a SAG mill. The simulation results suggest that the total charge load in the mill could be from 454 tonnes up to 510 tonnes, depending on the cone crusher's settings. All these simulation results presented in Figure 25 show that the cone crusher's settings have a significant impact on the mass flow in a SAG-cone circuit.

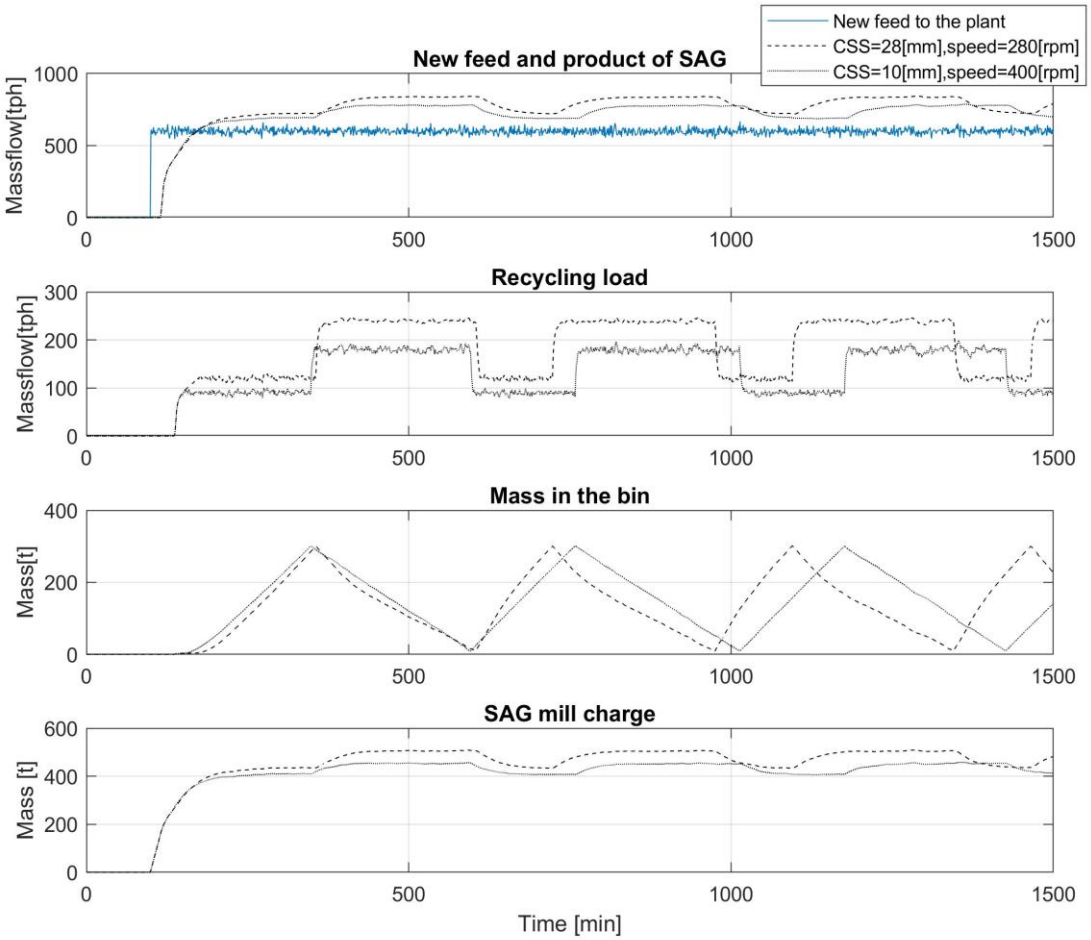

Figure 25. Simulation results from simulating scenario 2

The results in Paper B show that significant dynamic fluctuations can be induced by the cone crushers' on/off behavior. The cone crushers are thus acting as exciters of the circuit. Additionally, the cone crusher operating parameters, closed side setting and eccentric speed has a significant impact on the recycling load, the product tonnage, as well as PSD.

6 DISCUSSION

The aim of this chapter is to:

- Discuss the highlights and important conclusions drawn in this thesis.
- Answer the research questions proposed in Chapter 1.
- Discuss the future work concerning deeper analysis and new proposals that have been raised during this research work.

6.1 General Conclusions

The research presented in this thesis aims to understand the dynamic interactions between a SAG mill and its pebble crusher. The motivations underlying this work were to find a flexible, powerful, and efficient framework to predict and optimize the SAG mill grinding process with emphasis on different pebble crusher operational settings. Two main methodologies have been demonstrated for the overall objective.

The first modeling technique in Paper A and Paper B included a generic tumbling mill model based on a population balance framework where sub-processes like particle breakage, particle transportation, breakage appearance, and particle discharge are integrated. Meanwhile, dynamic models of cone crushers, conveyors, and screens were implemented for the plant circuit dynamic simulation. The results in Paper B showed that significant dynamic fluctuations in the whole grinding circuit could be induced by the pebble crusher operating parameters, CSS, and eccentric speed. Additionally, the hypothesis of increasing pebble crusher efficiency that, in turn, boosts the whole circuit performance has been validated with industrial data in Paper D.

The second method developed in Paper C incorporated several data-driven methods. A SAG mill power model was conducted with an ensemble method where the final predictor combined the weighted results from the individual predictor. Furthermore, the SAG mill power draw was considered to be a time series problem. The original dataset was reformatted by a sliding window and trained with an LSTM algorithm. This LSTM forecasting method took twenty-minute historical data and predicted a two-minute SAG mill power draw. Both the prediction

model and the time series forecasting model showed promising accuracy for SAG mill power draw estimation. The data-driven methods are flexible, easy to employ for suitable industrial datasets, and show a great advantage in calculating SAG power draw with rapidly changing conditions.

A general framework of data analysis method was presented in Paper D. The main purpose of this paper is to develop an approach that can step-by-step separate the influence of any arbitrary machinery or rock characteristic from the raw data on plant performance. This method helps one to extract key information that can potentially be used for future optimization and new machine design.

The impact of pebble crushing on grinding circuit performance was studied with data-driven methods in Paper D. The circuit performance variable (mill throughput) and crusher operating setting variables (crusher power and crusher specific energy) were clustered. The original dataset was then split into different categories according to clustering labels. Labeled data distributions then showed clear correlations between high crusher utilization and high mill throughput.

6.2 Answering Research Questions

RQ 1: What are the dynamic interactions between the SAG mill and the pebble crusher in a grinding process?

Answer: In Paper B, the dynamics of a SAG mill and its pebble crushers are studied using simulation tools that were built based on individual models for each machine. It is shown in Paper B that even with a constant feed rate to the circuit, the recycling load flow rate can be changed by altering the cone crusher settings. Simulation results indicated that if the recycling material is crushed down to a certain size class where they have a higher breakage rate, this leads to a higher SAG mill efficiency. For some more complex circuits where more than one pebble crusher are integrated, significant dynamic fluctuations can be caused by the pebble crushers switching on and off during the operations.

In Paper C, statistical analysis of the industrial data has been carried out to validate the proposed problem. In order to isolate the impact of pebble crusher operating settings, some variables that may affect mill performance have been investigated, such as fresh feed size, or were removed from the original dataset, such as data points with old mill liners. The quantitative results show that the SAG mill specific energy reduces from 7.5 kWh/t to 6.9 kWh/t with higher utilization of pebble crushing. Apparent correlations between circuit performance and pebble crusher utilization levels are observed.

RQ 2: What approach can be used to model these interactions and other internal dynamics for SAG mills and pebble crushers?

Answer: Two modeling techniques are presented in this thesis. Paper A and Paper B propose fundamental models based on physical principles. A population balance framework is implemented for a tumbling mill with sub-models that consider breakage and transportation. Fundamental dynamic models for cone crushers, conveyors, bins, and

screens are also formulated with mass balance, material tracking, and size reduction. The data structures within these modeling units are standardized, which allows for a flexible adaptation to any circuit.

One of the advantages of this fundamental modeling approach is the generality to a wide variety of plants. Models based on the underlying physics can provide adequate accuracy for new comminution circuits and insights into future machinery design and optimization.

The second approach introduced in Paper C uses several types of data-driven methods. The strengths and weaknesses of these methods are the opposite to those of fundamental models. The data-driven models can provide a more accurate prediction but cannot represent the mechanistic understandings of the physical processes. The flexibility of this approach allows one to find the complex nonlinear relations between some input variables and certain target outputs. Nevertheless, the accuracy of the method mainly depends on the training dataset it is fed with. This data set needs to be of high-quality with a minimum of missing or outlier data points. A real-time online monitoring system that keeps updating and training models is recommended.

RQ 3: How can the approaches proposed in the thesis be adapted and implemented in industrial applications?

Answer: Mining operations collect large amounts of data from multiple sources. However, this data is often neither systematically nor effectively analyzed for a better understanding of the process or used for process optimization (Suriadi et al., 2018). In Paper D, a data analysis framework is presented, and a case study of isolating the impact of a pebble crusher operating setting in a comminution circuit has been carried out. The proposed approach provides standardized steps to extract key information and allows one to narrow down the operating conditions to a specific plant to identify optimization potential.

The fundamental dynamic modeling method introduced in Paper A and Paper B can be used for the following applications in the comminution process: control system development, plant pre-design evaluation, maintenance planning, and operation optimization.

A large amount of data has been collected due to the extensive use of sensing technology and distributed control systems. It becomes more and more difficult to build first-principle models for the complex process (Ge et al., 2017). To effectively analyze data and adapt to the dynamic environment in industry, the following factors are essential for mineral processing engineers: mineral processing expertise and in-depth knowledge of the data analysis. In addition and more importantly, computational thinking is needed.

6.3 Future Work

Industrial tests and further model development are needed for future work. The main concerns within this research topic will focus on the following aspects:

- Further development of the fundamental models with high fidelity to implement the proposed simulation tools in a wider range of applications.
- Develop an online framework using data-driven methods where the models can be continuously updated based on the collection of real-time data. This can give more insights into process fault detection and wear monitoring.
- Formalize a modeling framework that combines data-driven methods and physics-based methods. Combining fundamental models with complex nonlinear machine learning algorithms has the potential for improved process modeling and optimization.
- Full-scale measurements need to be taken with different operating settings of a pebbles crusher in an AG/SAG circuit. Both crusher CSS and eccentric speed control should be considered.

References

ASBJÖRNSSON, G. 2015. *Crushing plant dynamics.* PhD Thesis, Chalmers University of Technology.

AUSTIN, L. G. & CHO, H. 2002. An alternative method for programming mill models. *Powder technology,* 122**,** 96-100.

BISHOP, C. M. 2006. *Pattern recognition and machine learning*, springer.

BREIMAN, L. 2001. Random forests. *Machine learning,* 45**,** 5-32.

CHOI, S. W., MORRIS, J. & LEE, I.-B. 2008. Dynamic model-based batch process monitoring. *Chemical Engineering Science,* 63**,** 622-636.

DE CARVALHO, M. 2013. Mechanistic modelling of semi-autogenous grinding. Center of Technology, UFRJ/COPPE. University of Rio de Janeiro.

DELANEY, G., MORRISON, R., SINNOTT, M., CUMMINS, S. & CLEARY, P. 2015. DEM modelling of non-spherical particle breakage and flow in an industrial scale cone crusher. *Minerals Engineering,* 74**,** 112-122.

DING, J., YANG, C. & CHAI, T. 2017. Recent progress on data-based optimization for mineral processing plants. *Engineering,* 3**,** 183-187.

EVERTSSON, C. M. 2000. *Cone crusher performance.* PhD Thesis, Chalmers University of Technology.

FUERSTENAU, M. C. & HAN, K. N. 2003. *Principles of mineral processing*, SME.

GE, Z. 2017. Review on data-driven modeling and monitoring for plant-wide industrial processes. *Chemometrics and Intelligent Laboratory Systems,* 171**,** 16-25.

GE, Z., SONG, Z., DING, S. X. & HUANG, B. 2017. Data mining and analytics in the process industry: The role of machine learning. *IEEE Access,* 5**,** 20590-20616.

GE, Z., SONG, Z. & GAO, F. 2013. Review of recent research on data-based process monitoring. *Industrial & Engineering Chemistry Research,* 52**,** 3543-3562.

GERS, F. A., SCHMIDHUBER, J. & CUMMINS, F. 1999. Learning to forget: Continual prediction with LSTM.

GRAVES, A., JAITLY, N. & MOHAMED, A.-R. Hybrid speech recognition with deep bidirectional LSTM. 2013 IEEE workshop on automatic speech recognition and understanding, 2013. IEEE, 273-278.

HAQUE, K. E. 1999. Microwave energy for mineral treatment processes—a brief review. *International journal of mineral processing,* 57**,** 1-24.

HASTIE, T., TIBSHIRANI, R., FRIEDMAN, J. & FRANKLIN, J. 2005. The elements of statistical learning: data mining, inference and prediction. *The Mathematical Intelligencer,* 27**,** 83-85.

HOCHREITER, S. & SCHMIDHUBER, J. 1997. Long short-term memory. *Neural computation,* 9**,** 1735-1780.

HORN, Z., AURET, L., MCCOY, J., ALDRICH, C. & HERBST, B. 2017. Performance of convolutional neural networks for feature extraction in froth flotation sensing. *IFAC-PapersOnLine,* 50**,** 13-18.

HOSEINIAN, F. S., FARADONBEH, R. S., ABDOLLAHZADEH, A., REZAI, B. & SOLTANI-MOHAMMADI, S. 2017. Semi-autogenous mill power model development using gene expression programming. *Powder technology,* 308**,** 61-69.

HULTHÉN, E. 2010. *Real-time optimization of cone crushers.* PhD Thesis, Chalmers University of Technology.

JIA, X., WILLARD, J., KARPATNE, A., READ, J., ZWART, J., STEINBACH, M. & KUMAR, V. Physics guided RNNs for modeling dynamical systems: A case study in simulating lake temperature profiles. Proceedings of the 2019 SIAM International Conference on Data Mining, 2019. SIAM, 558-566.

JNR, W. V. & MORRELL, S. 1995. The development of a dynamic model for autogenous and semi-autogenous grinding. *Minerals Engineering,* 8**,** 1285-1297.

JOHNSON, G., HUNTER, I. & HOLLE, H. 1994. Quantifying and improving the power efficiency of SAG milling circuits. *Minerals Engineering,* 7**,** 141-152.

KARPATNE, A., ATLURI, G., FAGHMOUS, J. H., STEINBACH, M., BANERJEE, A., GANGULY, A., SHEKHAR, S., SAMATOVA, N. & KUMAR, V. 2017a. Theory-guided data science: A new paradigm for scientific discovery from data. *IEEE Transactions on Knowledge and Data Engineering,* 29**,** 2318-2331.

KARPATNE, A., WATKINS, W., READ, J. & KUMAR, V. 2017b. Physics-guided neural networks (pgnn): An application in lake temperature modeling. *preprint :1710.11431*.

KOJOVIC, T., HILDEN, M., POWELL, M. & BAILEY, C. 2012. Updated Julius Kruttschnitt semi-autogenous grinding mill model.

LINDQVIST, M. & EVERTSSON, C. M. 2004. Improved flow-and pressure model for cone crushers. *Minerals engineering,* 17**,** 1217-1225.

LINDQVIST, M. & EVERTSSON, C. M. 2006. Development of wear model for cone crushers. *Wear,* 261**,** 435-442.

LIPPMANN, R. P. 1987. Anintroduction to computing with neural nets. *IEEE Assp magazine,* 4**,** 4-22.

LONG, Y., SHE, X. & MUKHOPADHYAY, S. 2018. HybridNet: integrating model-based and data-driven learning to predict evolution of dynamical systems. *arXiv preprint arXiv:1806.07439*.

MARINO, D. L., AMARASINGHE, K. & MANIC, M. Building energy load forecasting using deep neural networks. IECON 2016-42nd Annual Conference of the IEEE Industrial Electronics Society, 2016. IEEE, 7046-7051.

MAUGIS, C., CELEUX, G. & MARTIN‐MAGNIETTE, M. L. 2009. Variable selection for clustering with Gaussian mixture models. *Biometrics,* 65**,** 701-709.

MCCOY, J. & AURET, L. 2019. Machine learning applications in minerals processing: A review. *Minerals Engineering,* 132**,** 95-109.

MORRELL, S. 1992. The simulation of autogenous and semi-autogenous milling circuits. *Comminution: Theory and Practice***,** 369-380.

MORRELL, S. Power draw of wet tumbling mills and its relationship to charge dynamics. 2. An empirical approach to modelling of mill power draw. TRANSACTIONS OF THE INSTITUTION OF MINING AND METALLURGY SECTION C-MINERAL PROCESSING AND EXTRACTIVE METALLURGY, 1996. C54-C62.

MORRISON, R. & CLEARY, P. W. 2004. Using DEM to model ore breakage within a pilot scale SAG mill. *Minerals Engineering,* 17**,** 1117-1124.

NAPIER-MUNN, T. J., MORRELL, S., MORRISON, R. D. & KOJOVIC, T. 1996. *Mineral comminution circuits: their operation and optimisation*.

POWELL, M., EVERTSSON, C. M. & MAINZA, A. Redesigning SAG Mill Recycle Crusher Operation. SAG CONFERENCE 2019 VANCOUVER, 2019.

QUIST, J. & EVERTSSON, C. M. 2016. Cone crusher modelling and simulation using DEM. *Minerals Engineering,* 85**,** 92-105.

SURIADI, S., LEEMANS, S. J., CARRASCO, C., KEENEY, L., WALTERS, P., BURRAGE, K., TER HOFSTEDE, A. H. & WYNN, M. T. 2018. Isolating the impact of rock properties and operational settings on minerals processing performance: A data-driven approach. *Minerals Engineering,* 122**,** 53-66.

TANG, J., CHAI, T., ZHAO, L., YU, W. & YUE, H. 2012. Soft sensor for parameters of mill load based on multi-spectral segments PLS sub-models and on-line adaptive weighted fusion algorithm. *Neurocomputing,* 78**,** 38-47.

TANG, J., ZHAO, L., YU, W., YUE, H. & CHAI, T. 2010. Soft sensor modeling of ball mill load via principal component analysis and support vector machines. *Advances in Neural Network Research and Applications.* Springer.

TAYLOR, W. A. 2000. Change-point analysis: a powerful new tool for detecting changes.

TRUONG, C., OUDRE, L. & VAYATIS, N. 2018. ruptures: change point detection in Python. *arXiv preprint arXiv:1801.00826*.

WEINBERGER, K. Q., BLITZER, J. & SAUL, L. K. Distance metric learning for large margin nearest neighbor classification. Advances in neural information processing systems, 2006. 1473-1480.

WHITEN, W. 1974. A matrix theory of comminution machines. *Chemical Engineering Science,* 29**,** 589-599.

WITTEN, I. H., FRANK, E., HALL, M. A. & PAL, C. J. 2016. *Data Mining: Practical machine learning tools and techniques*, Morgan Kaufmann.

XING-YU, Q., PENG, Z., CHENGCHENG, X. & DONG-DONG, F. RNN-based Method for Fault Diagnosis of Grinding System. 2017 IEEE 7th Annual International Conference on CYBER Technology in Automation, Control, and Intelligent Systems (CYBER), 2017. IEEE, 673-678.

YU, P. 2017. *A generic dynamic model structure for tumbling mills.* PhD Thesis.

YU, P., XIE, W., LIU, L. & POWELL, M. Development of a dynamic mill model structure for tumbling mills. XXVII International Mineral Processing Congress-IMPC 2014 Conference Proceedings, 2014. Gecamin Digital Publications Santiago Chile, 41-51.

ZHANG, L., WANG, G. & GIANNAKIS, G. B. Real-time power system state estimation via deep unrolled neural networks. 2018 IEEE Global Conference on Signal and Information Processing (GlobalSIP), 2018. IEEE, 907-911.

ZHANG, Y. & HAGHANI, A. 2015. A gradient boosting method to improve travel time prediction. *Transportation Research Part C: Emerging Technologies,* 58**,** 308-324.